Studies with the Rhenacarborane $Cs[Re(CO)_3(\eta^5\text{-}7,8\text{-}C_2B_9H_{11})]$: Surprising Reactivity with a Range of Metal Ligand Fragments†

Dianne D. Ellis, Paul A. Jelliss, and F. Gordon A. Stone*

Department of Chemistry & Biochemistry, Baylor University, Waco, Texas 76798-7348

Received July 1, 1999

The rhenacarborane salt $Cs[Re(CO)_3(\eta^5\text{-}7,8\text{-}C_2B_9H_{11})]$ (**1**) has been synthesized in excellent yield using a new procedure. Treatment of CH_2Cl_2 solutions of **1** with $[RuCl_2(PPh_3)_3]$ yields the *exo-closo* complex $[Re(CO)_3(\eta^5\text{-}2,3,10\text{-}(\mu\text{-}H)_3\text{-}exo\text{-}\{RuCl(PPh_3)_2\}\text{-}7,8\text{-}C_2B_9H_8)]$ (**2a**). In this molecule a $[RuCl(PPh_3)_2]^+$ moiety is exopolyhedrally bound via three B−H⇀Ru bonds to a *closo*-3,1,2-ReC_2B_9 system. An X-ray diffraction study revealed that one of these agostic interactions utilizes a β-B−H bond in the coordinating CCB*B*B face of the cage, while the source of the remaining two B−H⇀Ru bonds is in the B_5 belt. The anion of salt **1** also binds exopolyhedral $[Rh(PPh_3)_2]^+$ and $[Rh\{Fe(\eta\text{-}C_5H_4PPh_2)_2\}]^+$ fragments in the complexes $[Re(CO)_3(\eta^5\text{-}5,10\text{-}(\mu\text{-}H)_2\text{-}exo\text{-}(RhL_2)\text{-}7,8\text{-}C_2B_9H_9)]$ (L_2 = $(PPh_3)_2$ (**3a**), $\{Fe(\eta\text{-}C_5H_4PPh_2)_2\}$ (**3b**)). Reaction of **1** with the salts $[M(CO)_2(THF)(\eta\text{-}C_5H_5)][BF_4]$ (M = Fe, Ru) and $[Fe(CO)_2(THF)(\eta\text{-}C_5Me_5)][BF_4]$ gives the complexes $[Re(CO)_3(\eta^5\text{-}n\text{-}(\mu\text{-}H)\text{-}exo\text{-}\{M(CO)_2(\eta\text{-}C_5R_5)\}\text{-}7,8\text{-}C_2B_9H_{10})]$ (M = Fe, R = H, n = 10 (**4a**); M = Ru, R = H, n = 10 (**4b**); M = Fe, R = Me, n = 10 (**4c**), 9 (**4d**)) with isomers **4c** and **4d** formed as an inseparable mixture. An X-ray structural study on **4b** revealed that there was no Re−Ru bond and that an *exo*-$[Ru(CO)_2(\eta\text{-}C_5H_5)]^+$ fragment is bound to the rhenacarboranyl anion by a single unsupported B−H⇀Ru interaction with an unusually long B−Ru distance (2.695(13) Å). The compounds $[ReM(\mu\text{-}10\text{-}H\text{-}\eta^5\text{-}7,8\text{-}C_2B_9H_{10})(CO)_3(PPh_3)]$ (M = Cu (**5a**), Ag (**5b**)) were isolated from the reaction of **1** with sources of the fragments $[M(PPh_3)]^+$ (M = Cu, Ag). X-ray structure determinations of both species **5** revealed the presence of direct Re−M (M = Cu, Ag) connectivities bridged by carborane β-B−H⇀M interactions. In solution the complexes **5** are highly dynamic on the NMR time scale, even at low (−90 °C) temperatures.

Introduction

Studies on the synthesis and especially the reactivity of metallacarborane complexes having *closo*-3,1,2-MC_2B_9 and *closo*-2,1-MCB_{10} core structures has attracted our attention in recent years for several reasons. Thus, reactions where exopolyhedral metal−metal bonds are formed have been a particularly productive topic for investigation because many of the new di- and trinuclear metal compounds obtained possess carborane cages which function as nonspectator ligands.[1] Several years ago during a preliminary investigation[2] of the rhenacarborane $Cs[Re(CO)_3(\eta^5\text{-}7,8\text{-}C_2B_9H_{11})]$ (**1**), first synthesized by Hawthorne and Andrews,[3] it came as some surprise to us that there was no propensity for this salt to react either with strong acids ($HBF_4{\cdot}Et_2O$, $HCl(Et_2O)$, CF_3CO_2H) or with sources of the fragment $[Au(PPh_3)]^+$. Failure of $[Au(PPh_3)]^+$ to afford a Re−Au species was especially surprising, as the gold reagent reacts with several other anionic metallacarboranes to form metal−metal bonds.[4] However, recently the monocarbon rhenacarborane $[N(PPh_3)_2]_2[Re(CO)_3(\eta^5\text{-}7\text{-}CB_{10}H_{11})]$ has been used as an effective precursor to novel bimetallic complexes with Re−Pt, Re−Pd, Re−Rh, and Re−Ir bonds,[5] and this has prompted us to reexamine the reactivity of compound **1**. Despite the negative results obtained in attempts to protonate and aurate **1**, we demonstrate herein that this reagent does in fact display unusual reactivity toward mid- to late-transition-metal reagents. Moreover, despite the absence of a reaction with $[Au(PPh_3)]^+$, we have used reactions between **1** and $[M(PPh_3)]^+$ (M = Cu, Ag) to

† The compounds described in this paper have a rhenium atom incorporated into a *closo*-1,2-dicarba-3-rhenadodecaborane structure. However, to avoid a complicated nomenclature for the complexes reported, and to relate them to the many known rhenium species with η-coordinated cyclopentadienyl ligands, we treat the cages as *nido*-11-vertex ligands with numbering as for an icosahedron from which the 12th vertex has been removed.

(1) (a) Stone, F. G. A. *Adv. Organomet. Chem.* **1990**, *31*, 53. (b) Brew, S. A.; Stone, F. G. A. *Adv. Organomet. Chem.* **1993**, *35*, 135. (c) Jelliss, P. A.; Stone, F. G. A. *J. Organomet. Chem.* **1995**, *500*, 307.

(2) Li, S.; Stone, F. G. A. Unpublished results.

(3) (a) Hawthorne, M. F.; Andrews, T. D. *J. Am. Chem. Soc.* **1965**, *87*, 2496. (b) Andrews, T. D.; Hawthorne, M. F.; Howe, D. V.; Pilling, R. L.; Pitts, D.; Reintjes, M.; Warren, L. F., Jr.; Wegner, P. A.; Young, D. C. *J. Am. Chem. Soc.* **1968**, *90*, 879.

(4) (a) Goldberg, J. E.; Stone, F. G. A. *Polyhedron* **1992**, *11*, 2841. (b) Pilotti, M. U.; Stone, F. G. A.; Topaloğlu, I. *J. Chem. Soc., Dalton Trans.* **1991**, 1355. (c) Carr, N.; Gimeno, M. C.; Goldberg, J. E.; Pilotti, M. U.; Stone, F. G. A.; Topaloğlu, I. *J. Chem. Soc., Dalton Trans.* **1990**, 2253. (d) Jeffery, J. C.; Jelliss, P. A.; Stone, F. G. A. *J. Chem. Soc., Dalton Trans.* **1994**, 25. (e) Batten, S. A.; Jeffery, J. C.; Jones, P. L.; Mullica, D. F.; Rudd, M. D.; Sappenfield, E. L.; Stone, F. G. A.; Wolf, A. *Inorg. Chem.* **1997**, *36*, 2570.

(5) (a) Blandford, I.; Jeffery, J. C.; Jelliss, P. A.; Stone, F. G. A. *Organometallics* **1998**, *17*, 1402. (b) Jeffery, J. C.; Jelliss, P. A.; Rees, L. H.; Stone, F. G. A. *Organometallics* **1998**, *17*, 2258.

10.1021/om9905097 CCC: $18.00
Publication on Web 10/28/1999

Table 1. Analytical and Physical Data

	compd	color	yield/%	ν_{max}(CO)[a] /cm^{-1}	anal./%[b] C	H
2a	[Re(CO)$_3$(η^5-2,3,10-(μ-H)$_3$-*exo*-{RuCl(PPh$_3$)$_2$}-7,8-C$_2$B$_9$H$_8$)]	red	30	2024 vs, 1933 s br	46.3 (46.3)	3.9 (3.9)
3a	[Re(CO)$_3$(η^5-5,10-(μ-H)$_2$-*exo*-{Rh(PPh$_3$)$_2$}-7,8-C$_2$B$_9$H$_9$)]	red	65	2018 vs, 1923 s br	[c]44.6 (45.2)	4.0 (3.9)
3b[d]	[Re(CO)$_3$(η^5-5,10-(μ-H)$_2$-*exo*-(Rh{Fe(η-C$_5$H$_4$PPh$_2$)$_2$})-7,8-C$_2$B$_9$H$_9$)]	red	58	2019 vs, 1923 s br		
4a	[Re(CO)$_3$(η^5-10-(μ-H)-*exo*-{Fe(CO)$_2$(η-C$_5$H$_5$)}-7,8-C$_2$B$_9$H$_{10}$)]	orange	98	2066 m, 2032 s, 2015 s, 1922 s br	24.9 (24.9)	2.7 (2.8)
4b	[Re(CO)$_3$(η^5-10-(μ-H)-*exo*-{Ru(CO)$_2$(η-C$_5$H$_5$)}-7,8-C$_2$B$_9$H$_{10}$)]	yellow	47	2077 m, 2032 s, 2015 s, 1920 s br	23.1 (23.1)	2.6 (2.6)
4c,d[e]	[Re(CO)$_3$(η^5-*n*-(μ-H)-*exo*-{Fe(CO)$_2$(η-C$_5$Me$_5$)}-7,8-C$_2$B$_9$H$_{10}$)]	orange	92	2047 m, 2014 s, 2005 sh,1917 s br	[f]29.0 (29.4)	3.8 (3.8)
5a	[ReCu(μ-10-H-η^5-7,8-C$_2$B$_9$H$_{10}$)(CO)$_3$(PPh$_3$)]	white	57	2027 vs, 1951 s, 1930 s	38.1 (37.9)	3.6 (3.6)
5b	[ReAg(μ-10-H-η^5-7,8-C$_2$B$_9$H$_{10}$)(CO)$_3$(PPh$_3$)]	white	63	2024 vs, 1943 vs, 1924 vs	[g]34.6 (34.6)	3.3 (3.3)

[a] Measured in CH_2Cl_2; medium-intensity broad bands observed at ca. 2550 cm^{-1} in the spectra of all the compounds are due to B−H absorptions. [b] Calculated values are given in parentheses. [c] Contains 1.0 mol equiv of CH_2Cl_2, confirmed by NMR. [d] Unstable; microanalysis unavailable. [e] Formed as an inseparable 1:1 mixture of isomers: n = 10 (**4c**), 9 (**4d**). [f] Contains 1.0 mol equiv of CH_2Cl_2, confirmed by NMR. [g] Contains 0.5 mol equiv of CH_2Cl_2, confirmed by X-ray structure.

form rhenium−copper and −silver complexes with metal−metal bonds.

Results and Discussion

The original synthesis of complex **1** was reported over 30 years ago,[3] and its X-ray structural characterization was described soon after.[6] By modifiying the original procedure (see Experimental Section), we have improved the yield of **1** from the reported 58% to over 90%, making it an attractive starting material for the synthesis of rhenacarborane complexes. A diffuse negative charge distribution within the *closo*-3,1,2-ReC$_2$B$_9$ cage is anticipated for the anion of **1**, as was found with the dianion [Re(CO)$_3$(η^5-7-CB$_{10}$H$_{11}$)]$^{2-}$,[5a] and this must at least partially account for the low basicity at the metal center. The initial agenda for studies with **1** involved examining reactions with those transition-metal reagents which have successfully given adducts with the carboranyl anions [*nido*-7,8-R$_2$-7,8-C$_2$B$_9$H$_{10}$]$^-$ (R = H, alkyl, aryl) and [*closo*-1-CB$_{11}$H$_{12}$]$^-$.

Recent work by Chizhevsky and co-workers[7] has shown that the carboranyl anion [*nido*-7,8-C$_2$B$_9$H$_{12}$]$^-$ on treatment with [RuCl$_2$(PPh$_3$)$_3$] forms the adduct [2,3,-10-(μ-H)$_3$-*exo*-{RuCl(PPh$_3$)$_2$}-*nido*-7,8-C$_2$B$_9$H$_9$] in which the cage framework behaves as a tridentate ligand toward the ruthenium center. With this in mind, complex **1** was treated with 1 equiv of [RuCl$_2$(PPh$_3$)$_3$], affording the product [Re(CO)$_3$(η^5-2,3,10-(μ-H)$_3$-*exo*-{RuCl(PPh$_3$)$_2$}-7,8-C$_2$B$_9$H$_8$)] (**2a**; Chart 1) in somewhat poor yield (Table 1). Although spectroscopic data (Tables 2 and 3) were useful in elucidating the nature of **2a**, its relative novelty prompted us to carry out an X-ray diffraction characterization. The pertinent bond lengths and angles are given in Table 4, and the molecule is shown in Figure 1. The absence of a Re−Ru bond is immediately apparent, and the zwitterionic nature of the molecule is realized: the anion of **1** is coordinated with a [RuCl(PPh$_3$)$_2$]$^+$ cation through the mediacy of three B−H⇀Ru bonds involving one B−H connectivity protruding from the β-position of the lower coordinating CCB*B*B belt (Ru−B(4) = 2.310(3) Å) and two from the

Chart 1

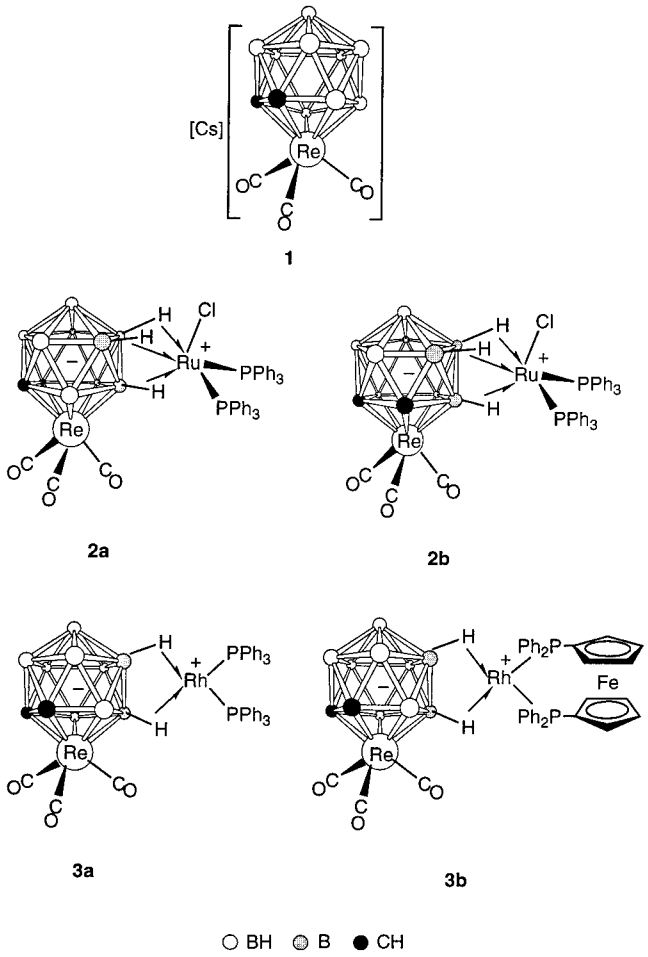

B$_5$ belt (Ru−B(9) = 2.379(3) Å, Ru−B(10) = 2.462(3) Å). This latter pair of interactions utilize both boron atoms antipodal to each of the cage carbon vertexes and are inequivalent. This might be attributed to subtle crystal packing forces, as later discussion of the NMR spectra will show that there is equivalence of the B$_5$ belt B−H⇀Ru contacts in solution. The PPh$_3$ ligands both lie transoid to the B$_5$ belt B−H⇀Ru agostic moieties (Ru−P(1) = 2.3093(7) Å, Ru−P(2) = 2.2870(8) Å, P(1)−Ru−H(9) = 169.7(8)°, P(2)−Ru−H(10) = 171.2(7)°) while the chloride ligand is transoid to the β-B(4)−H(4)⇀Ru system (Ru−Cl = 2.3189(7) Å, Cl−Ru−H(4) = 175.5-(9)°). The binding of the [RuCl(PPh$_3$)$_2$]$^+$ fragment to the

(6) Zalkin, A.; Hopkins, T. E.; Templeton, D. H. *Inorg. Chem.* **1966**, *5*, 1189.
(7) Chizhevsky, I. T.; Lobanova, I. A.; Bregadze, V. I.; Petrovskii, P. V.; Antonovich, V. A.; Polyakov, A. V.; Yanovskii, A. I.; Struchkov, Y. T. *Mendeleev Commun.* **1991**, 48.

Table 2. Hydrogen-1 and Carbon-13 NMR Data[a]

compd	^{1}H/δ[b]	^{13}C/δ[c]
2[d]	−15.56* [q br, 1 H, B−H→Ru, *J*(BH) = ca. 85], −14.84 [q br, 1 H, B−H→Ru, *J*(BH) = ca. 80], −4.76* [q br, 1 H, B−H→Ru, *J*(BH) = ca. 94], −4.63* [q br, 1 H, B−H→Ru, *J*(BH) = ca. 95], −3.52 [dq br 2 H, B−H→Ru, *J*(PH) = ca. 30, *J*(BH) = ca. 100], 2.91* (s br, 1 H, CH), 3.03 (s br, 2 H, CH), 3.09* (s br, 1 H, CH), 7.16−7.35 (m, 30 H, Ph)	194.6 (CO), 194.1* (CO), 137.8−128.2 (Ph), 33.1 (br, CH)
3a	−5.34 (m br, 1 H, B−H→Rh), 3.02 (s br, 2 H, CH), 7.14−7.36 (m, 30 H, Ph)	195.6 (CO), 135.5−128.3 (Ph), 33.8 (br, CH)
3b	−5.56 [q br, 1 H, B−H→Rh, *J*(BH) = ca. 80], 2.97 (s br, 2 H, CH), 4.20, 4.32 (m × 2, 8 H, PC_5H_4), 7.16−7.72 (m, 20 H, Ph)	195.7 (CO), 137.9−128.5 (Ph), 76.4 [dd, $C^1(PC_5H_4)$, *J*(PC) = 62, 3], 76.3 [AXX′, $C^2(PC_5H_4)$, *N* = 12[e]], 73.5 [AXX′, $C^3(PC_5H_4)$, *N* = 8[e]], 33.9 (br, CH)
4a	−19.67 [q br, 1 H, B−H→Fe, *J*(BH) = ca. 80], 2.92 (s br, 2 H, CH), 5.16 (s, 5 H, C_5H_5)	208.9 (FeCO), 196.1 (ReCO), 85.4 (C_5H_5), 33.3 (br, CH)
4b	−12.92 [q br, 1 H, B−H→Ru, *J*(BH) = 75], 2.96 (s br, 2 H, CH), 5.48 (s, 5 H, C_5H_5)	196.2 (ReCO), 194.3 (RuCO), 88.6 (C_5H_5), 33.4 (br, CH)
4c[f]	−18.46 (m br, 2 H, B−H→Fe), 1.81, 1.82 (s × 2, 30 H, C_5Me_5), 2.91 (s br, 2 H, CH), 2.94, 2.98 (s br × 2, 2 H, CH)	211.9 (FeCO × 2), 211.2, 211.1 (FeCO), 196.7, 196.4 (ReCO), 97.8, 97.3 (C_5Me_5), 34.6 (br, CH), 32.4 (br, CH × 2), 31.3 (br, CH), 10.0, 9.9 ($C_5\mathit{Me}_5$)
5a	3.34 (s br, 2 H, CH), 7.48−7.55 (m, 15 H, Ph)	191.1 (CO), 134.1 [d, C^2(Ph), *J*(PC) = 15], 131.7 [d, C^4(Ph), *J*(PC) = 2], 129.8 [d, C^1(Ph), *J*(PC) = 44], 129.7 [d, C^3(Ph), *J*(PC) = 10], 36.6 (br, CH)
5b	3.33 (s br, 2 H, CH), 7.49−7.56 (m, 15 H, Ph)	191.8 (CO), 134.2 [d, C^2(Ph), *J*(PC) = 16], 131.9 [d, C^4(Ph), *J*(PC) = 2], 129.8 [d, C^3(Ph), *J*(PC) = 11], 129.6 [d, C^1(Ph), *J*(PC) = 41], 36.2 (br, CH)

[a] Chemical shifts (δ) in ppm, coupling constants (*J*) in Hz, measurements at room temperature in CD_2Cl_2. [b] Resonances for terminal BH protons occur as broad unresolved signals in the range δ ca. −2 to 3. Resonances for cage CH and B−H→M protons are described as broad, corresponding to approximate $\nu_{1/2}$ values of 10 and 300 Hz, respectively. [c] Hydrogen-1 decoupled, chemical shifts are positive to high frequency of $SiMe_4$. Resonances for cage CH groups are described as broad, corresponding to an approximate $\nu_{1/2}$ value of 20 Hz. [d] Composed of a 15:1 mixture of isomers (see text). Peaks marked with an asterisk are due to the minor isomer. [e] Insufficient resolution prevents full analysis of coupling constants, $N = |J(AX) + J(AX')|$. [f] Composed of a 1:1 mixture of isomers (see text).

Table 3. Boron-11 and Phosphorus-31 NMR Data[a]

compd	^{11}B/δ[b]	^{31}P/δ[c]
2[d]	−5.6 (1 B), −10.2 (1 B), −12.3 [1 B, B−H→Ru, *J*(HB) = 76], −14.2* (1 B), −16.1* [1 B, B−H→Ru, *J*(HB) = 85], −19.0* (1 B), −20.3 (4 B), −26.1 (2 B)	57.4* [d, *J*(PP) = 20], 53.5, 43.8* [d, *J*(PP) = 20]
3a	−10.1 (1 B), −14.3 (6 B), −23.3 (2 B)	45.0 [d, *J*(RhP) = 187]
3b	−9.8 (1 B), −14.2 (6 B), −23.3 (2 B)	45.9 [d, *J*(RhP) = 194]
4a	−7.2 (1 B), −11.3 (2 B), −14.5 (2 B), −20.0 (1 B), −22.9 [1 B, B−H→Fe, *J*(HB) = 82], −23.7 (2 B)	
4b	−7.1 (1 B), −10.9 (2 B), −14.4 (2 B), −19.7 [1 B, B−H→Ru, *J*(HB) = 75], −23.6 (3 B)	
4c[e]	−7.1 (1 B), −8.3 (1 B), −11.2 (5 B), −15.1 (4 B), −20.3 (3 B), −23.9 (4 B)	
5a	−1.6 (1 B), −10.5 (2 B), −15.2 (3 B), −17.5 (1 B), −21.5 (2 B)	11.0
5b	−1.5 (1 B), −10.0 (2 B), −15.2 (2 B), −18.6 (2 B), −22.3 (2 B)	20.4 [d × 2, *J*(^{109}AgP) = 681, *J*(^{107}AgP) = 590]

[a] Chemical shifts (δ) in ppm, coupling constants (*J*) in Hz, measurements at room temperature in CD_2Cl_2. [b] Hydrogen-1 decoupled, chemical shifts are positive to high frequency of $BF_3{\cdot}OEt_2$ (external). The B−H→M assignments were made from fully coupled ^{11}B spectra. [c] Hydrogen-1 decoupled, chemical shifts are positive to high frequency of 85% H_3PO_4 (external). [d] Composed of a 15:1 mixture of isomers (see text). [e] Composed of a 1:1 mixture of isomers (see text). Peaks marked with an asterisk are due to the minor isomer.

rhenacarborane is thus strongly reminiscent of that observed for this moiety in [2,3,10-(μ-H)$_3$-*exo*-{RuCl(PPh$_3$)$_2$}-*nido*-7,8-$C_2B_9H_9$].[7] Similar tridentate bonding of a carborane to a transition-metal species has also been documented for the complex [7,8,12-(μ-H)$_3$-*exo*-{Zr(Me)$_2$(η-C_5Me_5)}-*closo*-1-$CB_{11}H_9$].[8] Further examination of the literature reveals that B−H→Ru interactions are in fact ubiquitous in metallaborane chemistry.[9] Indeed, a tridentate binding of a borane cage to a ruthenium fragment was reported for the complex [1,2,3-(μ-H)$_3$-*exo*-{RuCl(PPh$_3$)$_2$}-7-NEt$_3$-*closo*-$B_{12}H_8$] several years ago.[10] However, employment of a *closo*-metallacarborane in this tridentate role, namely that of **1**, is unprecedented. The Re(CO)$_3$ unit of **2a** is structurally unaffected by the exopolyhedral ruthenium moiety, displaying a piano stool arrangement with near-linear Re−C−O ligands (average Re−C−O = 177.0°).

In the IR spectrum there is a distinctive shift of ν_{max}(CO) signals to higher frequency from those in the starting material **1** (2005 and 1905 cm^{-1} in CH_2Cl_2) to those in the product **2** (2024 and 1933 cm^{-1}) (Table 1). This simply reflects the formation of a charge-compensated species from the anion of **1** but also is a good initial indicator that an adduct has formed in this and other reactions to be discussed presently. The ^{1}H NMR spectrum (Table 2) is highly informative with a low-field broad quartet at δ −14.84 which has the diagnostic coupling *J*(BH) ≈ 80 Hz.[1b] This may be assigned to the β-B(4)−H(4)→Ru proton. The remaining two B−H→Ru protons (H(9) and H(10)) give rise to a single but broad doublet of quartets at δ −3.52 corresponding to two protons. The quartet splitting (*J*(BH) = 100 Hz) is large for an agostic system but corresponds with the observa-

(8) Crowther, D. J.; Borkowski, S. I.; Swenson, D.; Meyer, T. Y.; Jordan, R. F. *Organometallics* **1993**, *12*, 2897.

(9) (a) Kennedy, J. D. *J. Chem. Soc., Dalton Trans.* **1993**, 2545 and references cited therein. (b) Teixidor, F.; Viñas, C.; Casabó, J.; Romerosa, A. M.; Rius, J.; Miravitlles, C. *Organometallics* **1994**, *13*, 914. (c) Viñas, C.; Nuñez, R.; Teixidor, F.; Kivekäs, R.; Sillanpää, R. *Organometallics* **1996**, *15*, 3850.

(10) Elrington, M.; Greenwood, N. N.; Kennedy, J. D.; Thornton-Pett, M. *J. Chem. Soc., Dalton Trans.* **1987**, 451.

Table 4. Selected Internuclear Distances (Å) and Angles (deg) for [Re(CO)$_3$(η^5-2,3,10-(μ-H)$_3$-*exo*-{RuCl(PPh$_3$)$_2$}-7,8-C$_2$B$_9$H$_8$)] (2a) with Estimated Standard Deviations in Parentheses

Re−C(3)	1.909(3)	Re−C(5)	1.920(4)	Re−C(4)	1.937(3)	Re−C(2)	2.332(3)
Re−C(1)	2.333(3)	Re−B(4)	2.336(3)	Re−B(5)	2.341(4)	Re−B(3)	2.347(3)
C(3)−O(3)	1.154(4)	C(4)−O(4)	1.149(3)	C(5)−O(5)	1.148(4)	B(4)−Ru	2.310(3)
B(9)−Ru	2.379(3)	B(10)−Ru	2.462(3)	H(4)−Ru	1.73(3)	H(9)−Ru	1.94(3)
H(10)−Ru	2.14(3)	Ru−P(2)	2.2870(8)	Ru−P(1)	2.3093(7)	Ru−Cl	2.3819(7)
P(1)−C(40)	1.831(3)	P(1)−C(20)	1.837(3)	P(1)−C(30)	1.848(3)	P(2)−C(60)	1.832(3)
P(2)−C(70)	1.832(3)	P(2)−C(50)	1.841(3)				
C(3)−Re−C(5)	89.88(14)	H(9)−Ru−P(2)	89.2(8)	C(5)−Re−B(3)	86.94(13)	C(5)−Re−B(4)	95.97(12)
C(3)−Re−C(2)	150.38(13)	H(9)−Ru−P(1)	169.7(8)	C(1)−Re−B(3)	72.31(12)	C(1)−Re−B(4)	71.87(11)
C(3)−Re−C(1)	109.77(13)	H(4)−Ru−Cl	175.5(9)	O(3)−C(3)−Re	176.8(3)	C(4)−Re−B(5)	133.80(13)
C(2)−Re−C(1)	40.88(11)	P(2)−Ru−Cl	91.49(3)	Ru−B(4)−Re	162.8(2)	B(4)−Re−B(5)	45.07(11)
C(4)−Re−B(4)	163.51(12)	C(3)−Re−C(4)	88.65(13)	H(10)−Ru−P(2)	171.2(7)	C(4)−Re−B(3)	119.33(12)
C(3)−Re−B(5)	85.87(13)	C(5)−Re−C(2)	119.74(13)	H(10)−Ru−P(1)	88.1(7)	B(4)−Re−B(3)	45.78(11)
C(2)−Re−B(5)	72.53(12)	C(5)−Re−C(1)	159.03(12)	H(9)−Ru−Cl	80.6(7)	O(4)−C(4)−Re	177.2(3)
C(3)−Re−B(3)	151.77(12)	C(3)−Re−B(4)	106.91(12)	P(1)−Ru−Cl	93.71(3)	H(4)−Ru−P(2)	89.8(9)
C(2)−Re−B(3)	42.09(11)	C(2)−Re−B(4)	71.89(10)	C(5)−Re−C(4)	89.35(13)	H(4)−Ru−P(1)	90.3(9)
B(5)−Re−B(3)	77.36(12)	C(5)−Re−B(5)	136.39(12)	C(4)−Re−C(2)	91.91(12)	P(2)−Ru−P(1)	99.54(3)
O(5)−C(5)−Re	176.6(3)	C(1)−Re−B(5)	42.68(11)	C(4)−Re−C(1)	98.09(12)	H(10)−Ru−Cl	92.3(7)

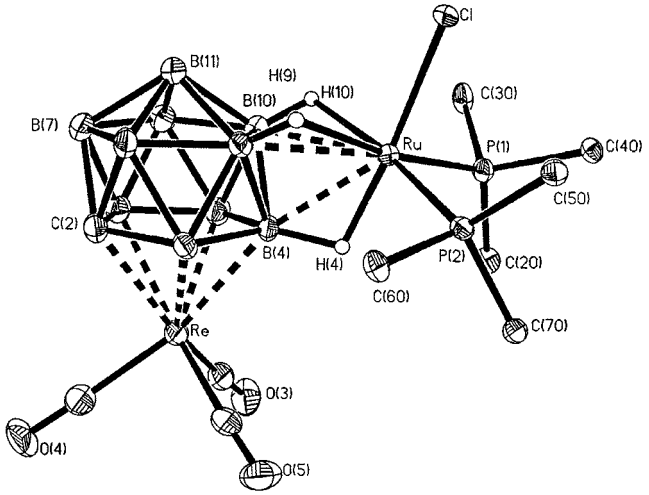

Figure 1. Structure of [Re(CO)$_3$(η^5-2,3,10-(μ-H)$_3$-*exo*-{RuCl(PPh$_3$)$_2$}-7,8-C$_2$B$_9$H$_8$)] (**2a**), showing the crystallographic labeling scheme. Thermal ellipsoids are shown at the 40% probability level. Only the agostic hydrogen and phenyl *ipso*-carbon atoms are shown for clarity.

tion in the X-ray structure that the B(9,10)−H(9,10)⇀Ru interactions are weaker than the B(4)−H(4)⇀Ru bond. This of course is a direct consequence of the stronger trans influence of the PPh$_3$ ligands compared with that of chloride.[9c] The signal at δ −3.52 shows a further discernible doublet splitting J(PH) ≈ 30 Hz, confirming the transoid location of the B(9,10)−H(9,10)⇀Ru protons with respect to the phosphines. With a resonance at δ 3.03 for the cage CH groups, the C_s symmetry of **2a** in solution is confirmed, with a mirror plane through the Re, Ru, Cl, and apical boron atoms. The ^{1}H NMR spectrum indicated the presence of the minor isomer **2b**, which is much less symmetrical, with three broad quartets at δ −15.56, −4.76, and −4.63 (J(BH) ≈ 85, 94, and 95 Hz, respectively) and two signals arising from the now inequivalent cage CH groups (δ 2.91 and 3.09). The relative peak integrals suggest a ratio of symmetrical **2a** to unsymmetrical **2b** of 15:1. The ^{31}P{^{1}H} NMR spectrum reflects the existence of **2a** with equivalent phosphine ligands (singlet at δ 53.5) and of **2b** with inequivalent PPh$_3$ groups (doublets at δ 43.8 and 57.4, J(PP) = 20 Hz). The ^{11}B{^{1}H} NMR spectrum shows principal peaks integrated in the ratio 1:1:1:4:2 due to **2a**. The resonance at δ −12.3 (1 B) becomes a doublet (J(HB) = 76 Hz) in the fully coupled ^{11}B NMR spectrum, while that at δ −26.1 (2 B) becomes a broader signal with irresolvable ^{1}H−^{11}B coupling. The former must be due to the β-boron atom B(4) in the CCB*B*B ring, while the latter likely arises from the two B$_5$ belt B(9,10) boron atoms. These chemical shift values are located at considerably higher field than is generally observed[1b] for species displaying exopolyhedral B−H⇀M bonds, and further discussion of this feature will be forthcoming. The ^{11}B and ^{11}B{^{1}H} NMR spectra also reveal weak resonances due to the minor species **2b**, though most are obscured by larger peaks for **2a**. Most notable for **2b**, though, is a resonance at δ −16.1 which becomes a doublet in the ^{11}B NMR spectrum with J(HB) = 85 Hz. It is proposed that this signal, which correlates with the resonance at δ −15.56 (J(BH) = 85 Hz) in the ^{1}H NMR spectrum, arises from the α-boron atom in the CC*B*BB ring. Thus, the minor isomer **2b** (Chart 1) employs three inequivalent agostic B−H⇀Ru interactions, one using the α-boron atom in the CC*B*BB belt and the other two from adjacent B$_5$ belt boron atoms (i.e. B(3), B(8), and B(9) if one employed the same crystallographic numbering scheme as in Figure 1 for **2a**). This is preferred over an alternative model invoking use of two CC*BB*B belt boron atoms and one from the B$_5$ ring, since this arrangement would place the chlorine atom in close proximity to the Re(CO)$_3$ carbonyl ligands. The ^{13}C{^{1}H} NMR spectrum of **2** displays a single sharp signal at δ 194.6 for the Re(CO)$_3$ carbonyl carbon nuclei of **2a** and a further singlet resonance for this group at δ 194.1 for **2b**. Thus, as for the parent complex **1**, the Re(CO)$_3$ unit in both isomers of **2** is rapidly spinning relative to the cage about an axis through the Re and apical boron atoms, thereby rendering the CO ligands equivalent on the NMR time scale.

Our interpretation of the NMR data for **2** contrasts with that given for the NMR data for the complex [2,3,10-(μ-H)$_3$-*exo*-{RuCl(PPh$_3$)$_2$}-*nido*-7,8-C$_2$B$_9$H$_9$],[7] which in solution was believed to be undergoing a systematic and reversible oxidative addition of the agostic B−H⇀Ru bonds to give various B−Ru−H moieties. We find no

such evidence for a similar process in complex **2** and propose that the minor isomer **2b** can be simply generated from **2a** by an effective lateral translation of the *exo*-$[RuCl(PPh_3)_2]^+$ fragment from one set of three deltahedrally arranged B−H vertexes on the cage surface to the adjacent set closer to the cage carbon atoms.

The NMR data for **2** imply that there is no significant dynamic behavior at ambient temperatures. This is in contrast with the previously reported behavior of the complexes [5,10-(μ-H)$_2$-*exo*-{Rh(PPh$_3$)$_2$}-7,8-Me$_2$-*nido*-7,8-$C_2B_9H_8$][11a] and [10-*endo*-{Au(PPh$_3$)}-5,10-(μ-H)$_2$-*exo*-{Rh(PPh$_3$)$_2$}-7,8-Me$_2$-*nido*-7,8-$C_2B_9H_7$],[11b] which have exopolyhedral $[Rh(PPh_3)_2]^+$ fragments bound via B−H⇀Rh interactions to carborane and auracarborane cages, respectively. In these molecules the rhodium fragments are dynamic with respect to the rest of the cage, rapidly exchanging B−H bonds around the cage surface at ambient temperatures. This prompted a study of the formation of related rhodium complexes using **1**. Treatment of the salt **1** with $[RhCl(PPh_3)_3]$ led to the isolation of the compound [Re(CO)$_3$(η^5-5,10-(μ-H)$_2$-*exo*-{Rh(PPh$_3$)$_2$}-7,8-$C_2B_9H_9$)] (**3a**; Chart 1) in reasonable yield (Table 1). The IR spectrum of the crude reaction mixture was consistent with the partial formation of **3a**, an adduct of the anion of **1**, and a rhodium−bisphosphine fragment. However, the presence of a third PPh_3 molecule, derived from $[RhCl(PPh_3)_3]$, gave rise to an equilibrium between **3a** and the salt $[Rh(PPh_3)_3][Re(CO)_3(\eta^5\text{-}7,8\text{-}C_2B_9H_{11})]$, a process also confirmed by NMR spectroscopy. The additional PPh_3 group was easily removed by several washings of the residue with light petroleum, leaving only product **3a**. Despite the instability of solutions of **3a**, which partially decomposed after 3−5 days, it was possible to collect interpretable NMR data (Tables 2 and 3).

The room-temperature ^{1}H NMR spectrum of **3a** shows a broad resonance at δ 3.02 typical for the cage CH groups, but also seen was a broad quartet at δ −5.34 integrated to one proton for a B−H⇀Rh group but with unresolved ^{11}B−^{1}H coupling. Similar observations were made for the above-mentioned dynamic complexes [5,10-(μ-H)$_2$-*exo*-{Rh(PPh$_3$)$_2$}-7,8-Me$_2$-*nido*-7,8-$C_2B_9H_8$] and [10-*endo*-{Au(PPh$_3$)}-5,10-(μ-H)$_2$-*exo*-{Rh(PPh$_3$)$_2$}-7,8-Me$_2$-*nido*-7,8-$C_2B_9H_7$].[11] The ^{11}B{^{1}H} NMR spectrum was regrettably unhelpful, comprising just three signals, one of which was integrated to six boron nuclei, and the ^{31}P{^{1}H} NMR spectrum contained a simple doublet at δ 45.0 with a coupling (J(RhP) = 187 Hz) typical for a Rh(PR$_3$)$_2$ unit in a cis square-planar configuration.[11] A variable-temperature NMR study was conducted, and it was found that at low temperatures the dynamic activity of **3a** could be significantly suppressed. A ^{31}P{^{1}H} NMR spectrum measured at −90 °C in CD_2Cl_2 (Figure 2) showed peaks due to the major species **A**, which appears to be an ABX system. The ^{103}Rh−^{31}P coupling constants (190 and 182 Hz) for the now-inequivalent phosphorus nuclei are discernible, but the system may not have fully decoalesced to be able to extract the J(PP) value. Thus, there may still be some mobility in the molecule at −90 °C, the lowest temperature attainable. This is supported by the ^{1}H NMR spectrum, also measured at −90 °C (Supporting Information), which displays a very broad quartet at δ −5.32 and a singlet at δ 3.00 with a peak integral ratio of 1:2. It is suggested that these peaks correspond to the tautomers **A** (Scheme 1), where the $[Rh(PPh_3)_2]^+$ fragment is anchored to the anion of **1** by a β-B−H⇀Rh interaction. It is also bound to the B_5 belt though a second B−H⇀Rh system involving one or other of the two boron atoms antipodal to a cage carbon, similar to that seen in the structures of [5,10-(μ-H)$_2$-*exo*-{Rh(PPh$_3$)$_2$}-7,8-Me$_2$-*nido*-7,8-$C_2B_9H_8$] and [10-*endo*-{Au(PPh$_3$)}-5,10-(μ-H)$_2$-*exo*-{Rh(PPh$_3$)$_2$}-7,8-Me$_2$-*nido*-7,8-$C_2B_9H_7$]. In CD_2Cl_2 solution at −90 °C there may still be rapid exchange of these adjacent HC-antipodal B−H bonds in the B_5 belt; i.e., the rhodium atom is flipping between these two B−H bonds. Thus, while the PPh_3 ligands are inequivalent, a time-averaged mirror plane of symmetry is generated in the molecule which encompasses the Re, Rh, the apical B, and both P atoms, which is sufficient to render the cage CH groups equivalent as observed. The minor species **B** is also present in solution at −90 °C. This gives rise to two signals in the

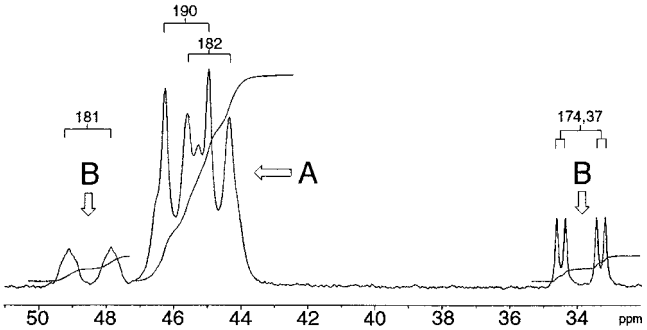

Figure 2. ^{31}P{^{1}H} NMR spectrum of compound **3a** in CD_2Cl_2 at −90 °C. Peaks labeled **A** and **B** are assigned to the molecules similarly labeled in Scheme 1.

Scheme 1. Pathways in the Dynamic Behavior of Complex 3a

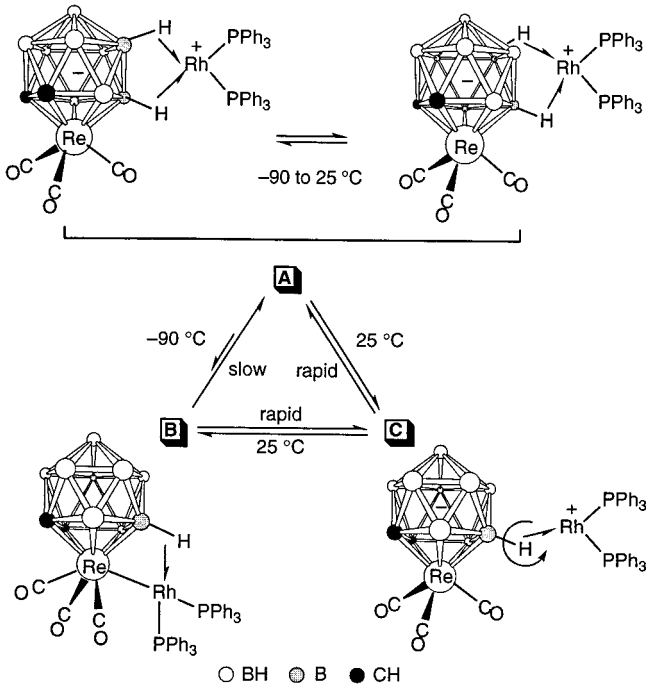

(11) (a) Long, J. A.; Marder, T. B.; Behnken, P. E.; Hawthorne, M. F. *J. Am. Chem. Soc.* **1984**, *106*, 2979. (b) Jeffery, J. C.; Jelliss, P. A.; Stone, F. G. A. *J. Chem. Soc., Dalton Trans.* **1993**, 1073.

^{31}P{^{1}H} NMR spectrum measured at this temperature (Figure 2): a broad doublet at δ 48.5 (J(RhP) = 181 Hz) and a much sharper doublet of doublets at δ 33.9 (J(RhP) = 174 Hz, J(PP) = 37 Hz). In the ^{1}H NMR spectrum at this temperature a broad quartet is seen at δ −8.26 (B−H⇀Rh) with a singlet at δ 3.16 (cage CH), these signals integrated in the ratio 1:2. This is very strong evidence for the species **B** (Scheme 1), which has a Re−Rh bond. The broadness of the doublet at δ 48.5 in the ^{31}P{^{1}H} NMR spectrum can be accounted for by assigning it to the PPh_3 ligand which lies transoid to the B−H⇀Rh interaction. Such broadening has been observed in similar molecules with a Pt(PR$_3$)$_2$ fragment bonded in this manner and is attributed to the trans location of the quadrupolar ^{11}B nucleus.[5a,12] The ratio of **A** to **B** is 4:1, as deduced from both the ^{1}H and ^{31}P{^{1}H} NMR spectra at −90 °C. The fact that molecules **A** and **B** can be observed at −90 °C implies that the Re−Rh bond formation/fission process has been decelerated to a rate slow enough on the NMR time scale to distinguish between the two species. At room temperature this process must be occurring rapidly enough that only the single β-B−H⇀Rh anchor can be observed in the ^{1}H NMR spectrum (δ −5.34, Table 2). The phosphorus nuclei are rendered equivalent most likely by virtue of the intermediacy of the species **C** (Scheme 1), where rapid rotation about the β-B−H⇀Rh system occurs, hence the observation of a lone doublet resonance in the room-temperature ^{31}P{^{1}H} NMR spectrum (δ 45.0, J(RhP) = 187 Hz; Table 3). Complex **C** must be a long-lived intermediate on the path between **A** and **B** but is unlikely to be the ground-state structure. On the basis of the prevalence of **A** at −90 °C and the previously determined structures of [5,10-(μ-H)$_2$-*exo*-{Rh(PPh$_3$)$_2$}-7,8-Me$_2$-*nido*-7,8-C$_2$B$_9$H$_8$] and [10-*endo*-{Au(PPh$_3$)}-5,-10-(μ-H)$_2$-*exo*-{Rh(PPh$_3$)$_2$}-7,8-Me$_2$-*nido*-7,8-C$_2$B$_9$H$_7$], the molecule **3a** shown in Chart 1 is the best representation.

In an attempt to form a more stable species in this class which might give X-ray-quality crystals, compound **1** was reacted with a source of the cationic fragment [Rh{Fe(η-C$_5$H$_4$PPh$_2$)$_2$}]$^+$ to give the complex [Re(CO)$_3$(η^5-5,10-(μ-H)$_2$-*exo*-(Rh{Fe(η-C$_5$H$_4$PPh$_2$)$_2$})-7,8-C$_2$B$_9$H$_9$)] (**3b**; Chart 1). While it was possible to measure spectroscopic data for **3b**, it proved to be even less stable than **3a**. It does, however, represent an interesting example of a metallacarborane incorporating first-, second-, and third-row transition metals, with no direct metal−metal bonds. The IR spectrum (Table 1) is identical with that of **3a**, and the ^{11}B{^{1}H} and ^{31}P{^{1}H} NMR spectra (Tables 2 and 3) are extremely similar. The ^{1}H NMR spectrum revealed a diagnostic broad quartet at δ −5.56, and this and the ^{13}C{^{1}H} NMR spectrum displayed the expected resonances for the equivalent η-C$_5$H$_4$PPh$_2$ rings. It is reasonable to assume that **3b** is undergoing the same dynamic processes in solution as **3a**.

The salt [Fe(CO)$_2$(THF)(η-C$_5$H$_5$)][BF$_4$] (THF = tetrahydrofuran) is a useful synthon and is easily formed by the reaction of [FeI(CO)$_2$(η-C$_5$H$_5$)] with AgBF$_4$ in THF.[13] Treatment of this iron salt with **1** gave [Re(CO)$_3$-(η^5-10-(μ-H)-*exo*-{Fe(CO)$_2$(η-C$_5$H$_5$)}-7,8-C$_2$B$_9$H$_{10}$)] (**4a**; Chart 2) in excellent yield (Table 1). The IR spectrum in the CO region (Table 1) with absorbances at 2015 and 1922 cm^{-1} (ν_{max}(ReCO)) and at 2066 and 2032 cm^{-1} (ν_{max}(FeCO)) clearly indicates that an adduct has formed and that the iron center is still cationic in nature. An interesting comparison may be made with the complex [12-μ-H-*exo*-{Fe(CO)$_2$(η-C$_5$H$_5$)}-*closo*-1-CB$_{11}$H$_{11}$] synthesized by Reed and co-workers,[14] where ν_{max}(FeCO) absorptions are observed at 2065 and 2026 cm^{-1} (KBr disk). This complex was characterized by an X-ray structural analysis, which revealed that the [*closo*-1-CB$_{11}$H$_{12}$]$^-$ anion was coordinated to the [Fe(CO)$_2$(η-C$_5$H$_5$)]$^+$ fragment through the B−H bond antipodal to the carbon vertex to give a zwitterionic species, having the positive charge localized on the iron center and the negative charge dispersed throughout the cage infrastructure. Unfortunately, there are little reported NMR data for this complex. The ^{1}H NMR spectrum of **4a** displayed a broad high-field resonance at δ −19.67 with an ^{11}B−^{1}H coupling that was barely observable (J(BH) ≈ 80 Hz). This coupling was more readily extracted from the fully coupled ^{11}B NMR spectrum, which showed a doublet at δ −22.9 (J(HB) = 82 Hz). The magnitude of the coupling constant is typical for a B−H⇀M system,[1b] but the chemical shifts for these signals in both the ^{1}H and ^{11}B NMR spectra are much further upfield than expected. It was noted above that a similar chemical shift regime was recognized in the NMR spectra of complex **2**. The range of chemical shifts normally encountered for these groups in complexes where there

Chart 2

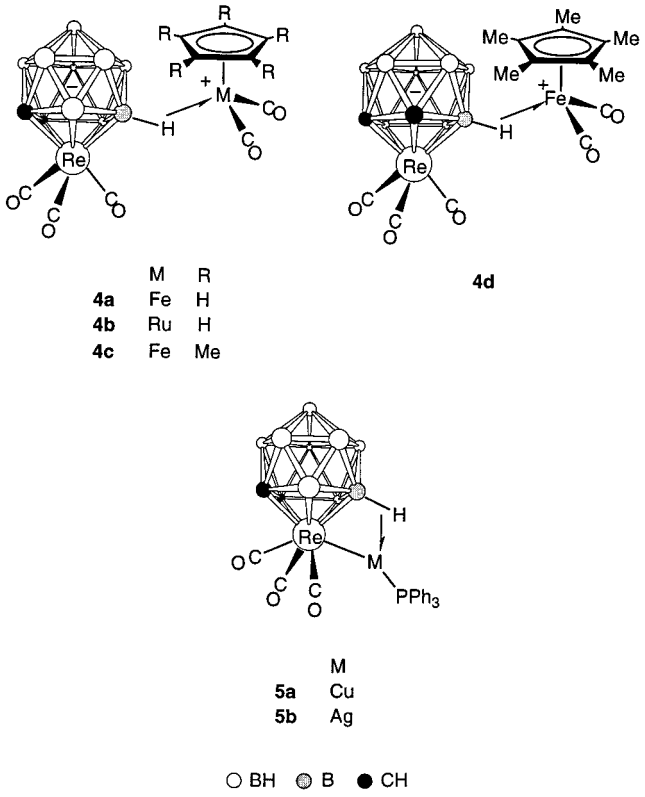

	M	R
4a	Fe	H
4b	Ru	H
4c	Fe	Me

4d

	M
5a	Cu
5b	Ag

(12) (a) Goldberg, J. E.; Mullica, D. F.; Sappenfield, E. L.; Stone, F. G. A. *J. Chem. Soc., Dalton Trans.* **1992**, 2693. (b) Devore, D. D.; Howard, J. A. K.; Jeffery, J. C.; Pilotti, M. U.; Stone, F. G. A. *J. Chem. Soc., Dalton Trans.* **1989**, 303. (c) Attfield, M. J.; Howard, J. A. K.; Jelfs, A. N. de M.; Nunn, C. M.; Stone, F. G. A. *J. Chem. Soc., Dalton Trans.* **1987**, 2219.

(13) Reger, D. L.; Coleman, C. *J. Organomet. Chem.* **1977**, *131*, 153.
(14) Liston, D. J.; Lee, Y. J.; Scheidt, W. R.; Reed, C. A. *J. Am. Chem. Soc.* **1989**, *111*, 6643.

Table 5. Selected Internuclear Distances (Å) and Angles (deg) for [Re(CO)$_3$(η^5-10-(μ-H)-*exo*-{Ru(CO)$_2$(η-C$_5$H$_5$)}-7,8-C$_2$B$_9$H$_{10}$)] (4b) with Estimated Standard Deviations in Parentheses

Re−C(3)	1.882(14)	Re−C(4)	1.886(14)	Re−C(5)	1.91(2)	Re−C(2)	2.301(12)
Re−C(1)	2.316(10)	Re−B(3)	2.343(12)	Re−B(5)	2.365(12)	Re−B(4)	2.397(12)
Re−Ru	4.4147(11)	C(3)−O(3)	1.171(13)	C(4)−O(4)	1.17(2)	C(5)−O(5)	1.15(2)
B(4)−H(4)	1.67(10)	B(4)−Ru	2.695(13)	Ru−C(7)	1.884(12)	Ru−C(8)	1.925(13)
Ru−H(4)	1.80(12)	Ru−C(23)	2.191(11)	Ru−C(24)	2.207(11)	Ru−C(21)	2.208(11)
Ru−C(20)	2.223(10)	Ru−C(22)	2.225(11)	C(7)−O(7)	1.133(13)	C(8)−O(8)	1.102(13)
C(3)−Re−C(4)	88.4(5)	C(23)−Ru−C(20)	62.0(4)	C(7)−Ru−C(23)	106.7(5)	C(4)−Re−B(4)	93.5(5)
C(3)−Re−C(2)	109.2(4)	H(4)−Ru−C(22)	130(3)	C(7)−Ru−C(24)	143.8(5)	O(4)−C(4)−Re	177.6(13)
C(3)−Re−C(1)	148.9(5)	C(23)−Ru−C(22)	36.8(4)	H(4)−Ru−C(21)	111(3)	Re−B(4)−Ru	120.1(5)
C(2)−Re−C(1)	40.4(4)	C(20)−Ru−C(22)	61.4(4)	C(23)−Ru−C(21)	61.7(4)	C(7)−Ru−C(8)	91.0(5)
C(5)−Re−B(3)	136.7(6)	O(8)−C(8)−Ru	174.1(11)	C(7)−Ru−C(20)	149.9(5)	C(8)−Ru−C(23)	101.8(5)
C(5)−Re−B(5)	118.0(6)	C(3)−Re−C(5)	88.5(6)	C(24)−Ru−C(20)	36.3(4)	C(8)−Ru−C(24)	93.1(5)
C(5)−Re−B(4)	162.4(5)	C(4)−Re−C(2)	159.8(5)	C(7)−Ru−C(22)	92.5(5)	C(7)−Ru−C(21)	112.9(5)
O(5)−C(5)−Re	176.5(14)	C(4)−Re−C(1)	122.7(4)	C(24)−Ru−C(22)	61.1(5)	C(24)−Ru−C(21)	61.1(4)
H(4)−Ru−C(7)	65(3)	C(3)−Re−B(3)	86.4(5)	H(4)−Ru−B(4)	37(3)	C(8)−Ru−C(20)	118.1(5)
H(4)−Ru−C(23)	166(3)	C(3)−Re−B(5)	153.4(5)	C(4)−Re−C(5)	90.5(7)	C(21)−Ru−C(20)	37.0(4)
H(4)−Ru−C(24)	151(3)	C(3)−Re−B(4)	108.8(5)	C(5)−Re−C(2)	99.5(5)	C(8)−Ru−C(22)	137.0(5)
C(23)−Ru−C(24)	37.3(4)	O(3)−C(3)−Re	175.9(11)	C(5)−Re−C(1)	91.1(5)	C(21)−Ru−C(22)	36.6(4)
C(8)−Ru−C(21)	153.6(5)	H(4)−B(4)−Ru	39(3)	C(4)−Re−B(3)	132.3(5)	O(7)−C(7)−Ru	176.7(11)
H(4)−Ru−C(20)	120(3)	H(4)−Ru−C(8)	89(3)	C(4)−Re−B(5)	88.2(5)		

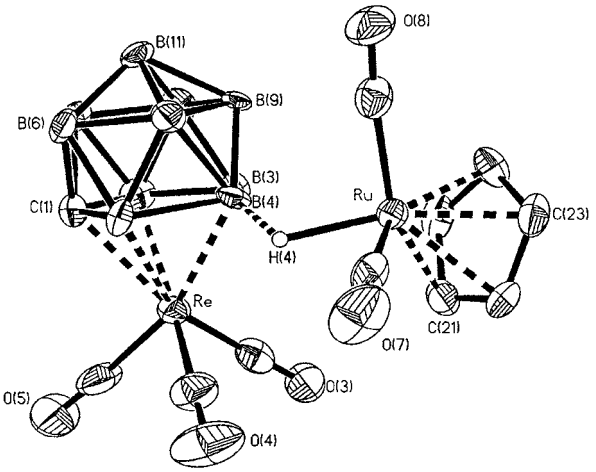

Figure 3. Structure of [Re(CO)$_3$(η^5-10-(μ-H)-*exo*-{Ru(CO)$_2$-(η-C$_5$H$_5$)}-7,8-C$_2$B$_9$H$_{10}$)] (**4b**), showing the crystallographic labeling scheme. Thermal ellipsoids are shown at the 40% probability level. Only the agostic hydrogen atom is shown for clarity.

is a core M(B−H⇀M′) architecture, i.e., a metal−metal bond bridged by a single carborane B−H bond, are δ −5 to −11 (^{1}H) and δ 10−30 (^{11}B).[1b] Thus, it seemed likely that there was no Re−Fe bond in complex **4a**, an idea supported by the observation in the ^{13}C{^{1}H} NMR spectrum of just two resonances due to CO ligands (δ 208.9 (FeCO × 2) and 196.1 (ReCO × 3)). It was not possible to grow tractable crystals of **4a**, but the ruthenium analogue [Re(CO)$_3$(η^5-10-(μ-H)-*exo*-{Ru(CO)$_2$-(η-C$_5$H$_5$)}-7,8-C$_2$B$_9$H$_{10}$)] (**4b**, Chart 2) was prepared and suitable crystals harvested for a structure determination. Selected bond lengths and angles are given in Table 5, and the molecule is shown in Figure 3.

The absence of a Re−Ru bond is confirmed, as is the participation of the β-B−H bond in ligating the ruthenium atom. The exact nature of B−H⇀M bonding and the associated B−M distances might be expected to reflect whether a B−H⇀M interaction is bridging a metal−metal bond or is in fact an unsupported or isolated group. Kennedy[9a] reports a range of Ru−B bond distances for B−H⇀Ru groups in a collection of many ruthenaboranes, the longest of which is 2.484(12) Å. In complex **2** the longest such distance is 2.462(3) Å (B(10)−Ru; Table 4), while that in the complex [RuW-(μ-CC$_6$H$_4$Me-4)(CO)$_3$(η-C$_5$H$_5$)(η^5-7,8-Me$_2$-7,8-C$_2$B$_9$H$_9$)], in which a carborane bridges a Ru−W bond via a B−H⇀Ru group, is 2.400(9) Å.[15] The B(4)−Ru distance in **4b** (2.695(13) Å) is therefore extremely long, and the absence of a bond between these two atoms is justified in Figure 3. The proton H(4) was located in final difference Fourier maps with the distances Ru−H(4) = 1.80(12) and B(4)−H(4) = 1.67(10) Å. While it is realized that even for high-quality structures (R1 < 0.05) values for bond distances involving hydrogen atoms are considered tenuous at best, the B(4)−H(4) contact in **4b** is notably long. Thus, the B−H distance in the B−H⇀Ru linkage in [RuW(μ-CC$_6$H$_4$Me-4)(CO)$_3$(η-C$_5$H$_5$)(η^5-7,8-Me$_2$-7,8-C$_2$B$_9$H$_9$)] is 1.33 Å, which is usual.[15] Hence, complex **4b** almost has the appearance of a [RuH(CO)$_2$-(η-C$_5$H$_5$)] molecule loosely bound to a neutral [Re(CO)$_3$-(η^5-7,8-C$_2$B$_9$H$_{10}$)] species at the β-boron position in the CCB*B*B ring, though such a relatively exposed boron vertex is difficult to envision. Indeed, **4b** could be viewed as a product of incipient hydride extraction, a process that, upon completion, has precedence in several areas of metallacarborane chemistry.[16] The carbonyl ligands of **4b** are nearly linear (average Re−C−O = 176.7°, average Ru−C−O = 175.4°), and the spatial arrangements of ligands around the metal centers is unremarkable, with both the carborane cage and cyclopentadienyl ligands η^5-coordinated to the rhenium and ruthenium atoms, respectively.

The NMR spectra of **4b** are akin to those of **4a**. In particular, the fully coupled ^{11}B NMR spectrum displays a doublet at δ −19.7 (J(HB) = 75 Hz), and the ^{1}H NMR spectrum has a broad quartet at δ −12.92 (J(BH) = 75 Hz) due to the β-B−H⇀Ru boron and proton nuclei, respectively. In solutions of both **4a** and **4b** a mirror plane can be generated by free rotation about the

(15) Green, M.; Howard, J. A. K.; Jelfs, A. N. de M.; Johnson, O.; Stone, F. G. A. *J. Chem. Soc., Dalton Trans.* **1987**, 73.
(16) (a) Mullica, D. F.; Sappenfield, E. L.; Stone, F. G. A.; Woollam, S. F. *Organometallics* **1994**, *13*, 157. (b) Gómez-Saso, M.; Mullica, D. F.; Sappenfield, E. L.; Stone, F. G. A. *Polyhedron* **1996**, *15*, 793. (c) Hendershot, S. L.; Jeffery, J. C.; Jelliss, P. A.; Mullica, D. F.; Sappenfield, E. L.; Stone, F. G. A. *Inorg. Chem.* **1996**, *35*, 6561.

B−H→M system, this being a consequence of the involvement of the CCB*B*B β-boron atom as opposed to one of the two possible α-borons in the CC*B*BB ring.

Kennedy has observed[9a] that there appears to be little correlation between the ^{1}H chemical shift values for B−H→Ru groups in metallaboranes and their Ru−B distances or the ligand disposition about the ruthenium atom. Where the possibility exists for a metal−metal bond to form, as we might have imagined in complex **4b** (or indeed **4a**), we believe it can be inferred from the significantly high field signals in the ^{1}H and ^{11}B NMR spectra emanating from these B−H→Ru groups that the [Re(CO)$_3$] and [Ru(CO)$_2$(η-C$_5$H$_5$)] fragments in fact remain unconnected by a Re−Ru bond in solutions of these compounds. Thus, the latter moiety functions exclusively as an exopolyhedral group bound by a single unsupported B−H→Ru interaction. The bonding to the carborane cage of the [Ru(CO)$_2$(η-C$_5$H$_5$)] fragment in **4b** is, however, atypical when compared with previously reported molecules with B−H→Ru groups. Whether this unorthodox bonding is extended to **4a** such that an [FeH(CO)$_2$(η-C$_5$H$_5$)] molecule is stabilized by a [Re(CO)$_3$(η^5-7,8-C$_2$B$_9$H$_{10}$)] unit remains speculative without firm structural proof but is interesting when one recalls that [FeH(CO)$_2$(η-C$_5$H$_5$)] readily decomposes to give the binuclear complex [Fe$_2$(μ-CO)$_2$(CO)$_2$(η-C$_5$H$_5$)$_2$] and H$_2$.[17]

A variation on the synthetic methodology which afforded **4a** and **4b** involved employing the salt [Fe(CO)$_2$(THF)(η-C$_5$Me$_5$)][BF$_4$], formed in situ from [FeI(CO)$_2$(η-C$_5$Me$_5$)] and AgBF$_4$ in THF, and reacting it with **1**. The product isolated was an inseparable 1:1 mixture of the two isomers [Re(CO)$_3$(η^5-*n*-(μ-H)-*exo*-{Fe(CO)$_2$(η-C$_5$Me$_5$)}-7,8-C$_2$B$_9$H$_{10}$)] (n = 10 (**4c**), 9 (**4d**); Chart 2). This was not immediately apparent from the IR spectrum (Table 1), which displays absorbances similar in form to that for **4a**, but shifted to lower frequency, particularly the ν_{max}(FeCO) peaks (2047 and 2014 cm^{-1}). This latter feature is no doubt due to the stronger donor ability of the η-C$_5$Me$_5$ ligand compared with η-C$_5$H$_5$. A broad quartet is observed in the ^{1}H NMR spectrum (Table 2) at δ −18.46, which is actually a composite of two B−H→Fe proton resonances, although a structure similar to **4a** is indicated. This is accompanied by the appearance of two singlets for the η-C$_5$Me$_5$ ligands in each isomer (δ 1.81 and 1.82) and, more importantly, three cage CH resonances at δ 2.91, 2.94, and 2.98 integrated in the ratio 2:1:1. The former signal (δ 2.91) arises from an isomer utilizing the β-boron atom in the CCB*B*B coordinating cage face to form the B−H→Fe bridge. The symmetrical structure **4c** results after allowing for free rotation in solution of the [Fe(CO)$_2$(η-C$_5$Me$_5$)] fragment about the B−H→Fe linkage and is precisely analogous to **4a**. This also gives rise to one FeCO resonance in the ^{13}C{^{1}H} NMR spectrum at δ 211.9 and one CH signal at δ 32.4. The second isomer **4d** lacks the mirror plane present in **4c**. This is most likely due to the α-boron atom in the CC*B*BB coordinating cage face being employed in the exopolyhedral linkage to the iron center. Thus, both the cage CH groups and the FeCO carbonyl ligands are rendered diastereotopic with resonances at δ 2.94 and 2.98 (^{1}H, CH), at δ 34.6 and 31.3 (^{13}C{^{1}H}, CH), and at δ 211.2 and 211.1 (^{13}C{^{1}H}, FeCO). The ^{11}B{^{1}H} and ^{11}B NMR spectra of **4c,d** contain broad overlapping peaks which were unfortunately not as informative as those of **4a** and **4b**.

Scheme 2[a]

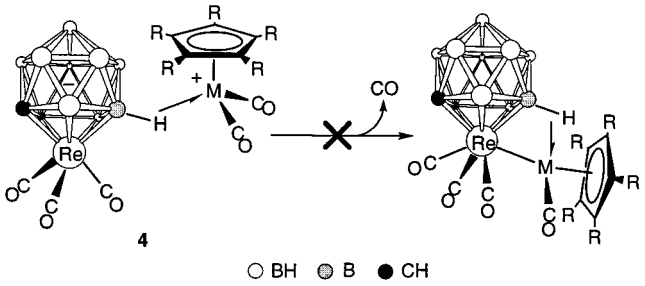

[a] Loss of CO from the complexes **4** could afford products with Re−Fe (or Ru) bonds, but this process was not observed.

It had been hoped that the compounds **4** would be precursors to stable complexes with Re−M (M = Fe, Ru) bonds resulting from the loss of a CO ligand from the iron or ruthenium centers. Solutions of these complexes were heated in various solvents and also treated with Me$_3$NO under differing conditions in order to promote ejection of a CO molecule as CO$_2$, but no new Re−M-bonded complexes could be identified (Scheme 2). In fact, these procedures invariably led to the regeneration of the anion of **1**.

The ability of M^I (M = Cu, Ag) metal centers to extend their coordination number beyond 2 is a feature more frequently encountered than in Au^I chemistry, due to the higher energy of gold 6p orbitals, which may not be included in the frontier set.[18] This observation encouraged us to examine the reactivity of **1** with sources of the fragments [M(PPh$_3$)]$^+$ (M = Cu, Ag) in the hope that where gold had failed, copper and/or silver might succeed. Treatment of **1** with either [CuCl(PPh$_3$)$_3$], or AgBF$_4$ in the presence of 1 equiv of PPh$_3$, gave the complexes [ReM(μ-10-H-η^5-7,8-C$_2$B$_9$H$_{10}$)(CO)$_3$(PPh$_3$)] (M = Cu (**5a**), Ag (**5b**); Chart 2). Both products form as a white powder or colorless crystals and have similar IR spectra (Table 1) which clearly indicate the formation of adducts. However, the information gleaned from the NMR spectra gave little clue as to the exact structural nature of these complexes. The ^{1}H and ^{13}C{^{1}H} NMR spectra were very straightforward with single resonances for the cage CH (δ 3.34 (**5a**), 3.33 (**5b**), ^{1}H; δ 36.6 (**5a**), 36.2 (**5b**), ^{13}C{^{1}H}) and CO (δ 191.1 (**5a**), 191.8 (**5b**)) groups (Table 2). There were no indications in the room-temperature ^{1}H NMR spectra of these molecules of any B−H→M interactions. The ^{31}P{^{1}H} NMR spectra (Table 3) each showed simple resonances with a singlet at δ 11.0 for **5a** and a pair of doublets at δ 20.4 for **5b**, this with the customary ^{107}Ag−^{31}P and ^{109}Ag−^{31}P couplings of 590 and 681 Hz, respectively.[19] The ^{11}B-{^{1}H} NMR spectra were similar but not identical, each with a set of five signals (1:2:3:1:2 (**5a**), 1:2:2:2:2 (**5b**)) for the BH groups, all of which displayed typical

(17) Green, M. L. H.; Street, C. N.; Wilkinson, G. *Z. Naturforsch.* **1959**, *14B*, 738.

(18) (a) Evans, D. G.; Mingos, D. M. P. *J. Organomet. Chem.* **1982**, *232*, 171. (b) Hamilton, E. J.; Welch, A. J. *Polyhedron* **1990**, *9*, 2407.

(19) Muetterties, E. L.; Alegranti, C. W. *J. Am. Chem. Soc.* **1972**, *94*, 6386.

Table 6. Selected Internuclear Distances (Å) and Angles (deg) for [ReCu(μ-10-H-η^5-7,8-$C_2B_9H_{10}$)(CO)$_3$(PPh$_3$)] (5a) with Estimated Standard Deviations in Parentheses

Re−C(3)	1.927(3)	Re−C(4)	1.927(3)	Re−C(5)	1.945(3)	Re−C(1)	2.296(3)
Re−C(2)	2.298(3)	Re−B(5)	2.352(3)	Re−B(3)	2.362(3)	Re−B(4)	2.381(3)
Re−Cu	2.6583(6)	C(3)−O(3)	1.147(3)	C(4)−O(4)	1.154(3)	O(5)−C(5)	1.148(3)
B(4)−Cu	2.169(3)	H(4)−Cu	1.67(3)	Cu−P	2.2051(8)		
C(3)−Re−C(4)	95.53(12)	O(3)−C(3)−Re	174.7(3)	C(3)−Re−Cu	76.71(8)	C(5)−Re−B(5)	129.18(12)
C(3)−Re−C(1)	108.87(12)	Cu−B(4)−Re	71.33(10)	C(1)−Re−Cu	121.01(7)	C(5)−Re−B(3)	123.55(12)
C(3)−Re−C(2)	150.26(12)	H(4)−Cu−Re	92.3(10)	B(3)−Re−Cu	77.74(8)	C(4)−Re−B(4)	103.09(11)
C(3)−Re−B(5)	85.65(12)	C(3)−Re−C(5)	85.53(12)	O(4)−C(4)−Re	175.4(3)	C(4)−Re−Cu	66.09(8)
C(3)−Re−B(3)	150.89(11)	C(4)−Re−C(1)	155.49(12)	H(4)−Cu−P	129.5(10)	C(2)−Re−Cu	118.61(7)
B(5)−Re−B(3)	76.87(12)	C(4)−Re−C(2)	113.81(12)	B(4)−Cu−Re	58.05(8)	B(4)−Re−Cu	50.61(8)
C(5)−Re−B(4)	164.89(11)	C(4)−Re−B(5)	145.98(11)	C(4)−Re−C(5)	84.71(12)	O(5)−C(5)−Re	178.4(3)
C(5)−Re−Cu	143.64(9)	C(4)−Re−B(3)	86.66(12)	C(5)−Re−C(1)	94.62(11)	B(4)−Cu−P	161.88(9)
B(5)−Re−Cu	81.29(8)	C(3)−Re−B(4)	106.27(12)	C(5)−Re−C(2)	92.20(11)	P−Cu−Re	137.25(3)

Table 7. Selected Internuclear Distances (Å) and Angles (deg) for [ReAg(μ-10-H-η^5-7,8-$C_2B_9H_{10}$)(CO)$_3$(PPh$_3$)] (5b) with Estimated Standard Deviations in Parentheses

Re−C(3)	1.87(2)	Re−C(5)	1.907(14)	Re−C(4)	1.918(13)	Re−C(1)	2.296(11)
Re−C(2)	2.316(11)	Re−B(3)	2.335(14)	Re−B(5)	2.337(13)	Re−B(4)	2.443(14)
Re−Ag	2.9344(12)	C(3)−O(3)	1.181(13)	C(4)−O(4)	1.156(13)	C(5)−O(5)	1.171(14)
B(4)−Ag	2.449(14)	H(4)−Ag	1.78(9)	Ag−P	2.373(3)		
C(3)−Re−C(5)	93.4(5)	O(4)−C(4)−Re	178.4(12)	C(5)−Re−Ag	70.2(4)	C(3)−Re−B(3)	134.3(5)
C(3)−Re−C(1)	122.2(5)	P−Ag−B(4)	171.1(3)	C(2)−Re−Ag	108.7(3)	C(4)−Re−B(5)	112.7(5)
C(3)−Re−C(2)	160.4(5)	H(4)−Ag−P	150(3)	B(4)−Re−Ag	53.2(3)	C(4)−Re−B(4)	157.6(5)
C(5)−Re−B(3)	90.6(5)	C(3)−Re−C(4)	86.6(5)	O(5)−C(5)−Re	176.6(11)	C(4)−Re−Ag	146.3(4)
C(3)−Re−B(5)	88.9(5)	C(5)−Re−C(1)	143.7(5)	P−Ag−Re	134.74(8)	B(3)−Re−Ag	66.7(4)
C(3)−Re−B(4)	94.6(5)	C(5)−Re−C(2)	105.3(5)	H(4)−Ag−Re	74(3)	O(3)−C(3)−Re	175.4(11)
C(3)−Re−Ag	72.1(4)	C(4)−Re−B(3)	139.1(5)	C(5)−Re−C(4)	85.9(5)	Re−B(4)−Ag	73.7(4)
C(1)−Re−Ag	124.2(3)	C(5)−Re−B(5)	161.3(5)	C(4)−Re−C(1)	89.1(5)	B(4)−Ag−Re	53.0(3)
B(5)−Re−Ag	93.1(4)	C(5)−Re−B(4)	116.3(5)	C(4)−Re−C(2)	100.1(5)		

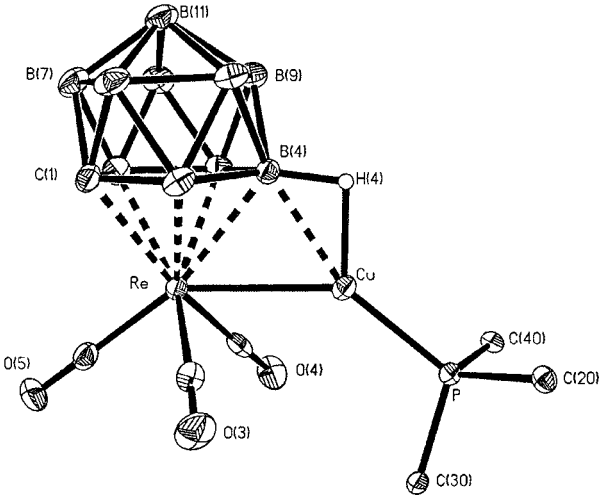

Figure 4. Structure of [ReCu(μ-10-H-η^5-7,8-$C_2B_9H_{10}$)(CO)$_3$(PPh$_3$)] (**5a**), showing the crystallographic labeling scheme. Thermal ellipsoids are shown at the 40% probability level. Only the agostic hydrogen and phenyl *ipso*-carbon atoms are shown for clarity.

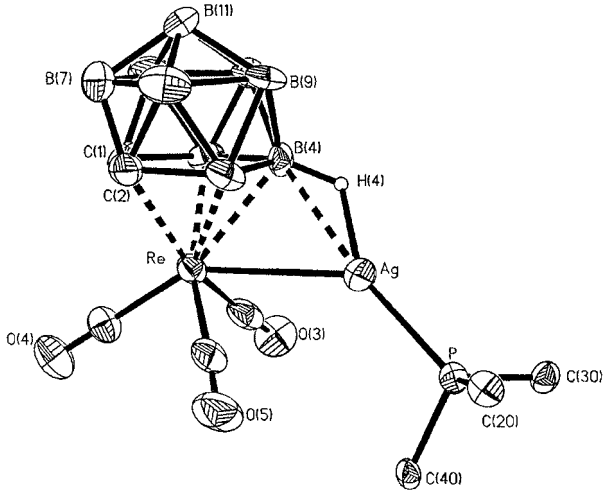

Figure 5. Structure of [ReAg(μ-10-H-η^5-7,8-$C_2B_9H_{10}$)(CO)$_3$(PPh$_3$)] (**5b**), showing the crystallographic labeling scheme. Thermal ellipsoids are shown at the 40% probability level. Only the agostic hydrogen and phenyl *ipso*-carbon atoms are shown for clarity.

coupling in the fully coupled ^{11}B NMR spectra as expected for terminal hydrogen atoms (J(HB) = 100−160 Hz).

Because of this seemingly inadequate information, X-ray crystal structure determinations were carried out on both **5a** and **5b**. Selected bond lengths and angles are given in Tables 6 (**5a**) and 7 (**5b**), and the molecules are displayed in Figures 4 (**5a**) and 5 (**5b**). The immediately apparent feature in each of these structures is the presence of direct Re−Cu (2.6583(6) Å) and Re−Ag (2.9344(12) Å) bonds. The Re−Cu distance is slightly longer than those found in [$Re_2Cu(\mu$-H)(H)$_4$(PMePh$_2$)$_6$][PF_6] (2.607(2) Å)[20a] and [$Re_2Cu_2(\mu$-I)$_2$(H)$_2(\eta$-$C_5H_5)_4$] (2.599(3) Å)[20b] but comparable with those in the complex [$Re_2Cu(\mu$-PCy$_2$)(CO)$_8$(PPh$_3$)] (average 2.673 Å).[20c] In the Cambridge Crystallographic Data Centre there are just two reports of X-ray diffractomeric studies for complexes with Re−Ag bonds: [NEt_3]$_5$[{Re_7AgC(CO)$_{21}$}$_2$Br], which contains a Re_3 face capped by an Ag atom (mean Re−Ag distance 2.882 Å),[21a] and [Ag{ReH_7(PPhPr$^i_2$)$_2$}$_2$][PF_6] (Re−Ag = 2.838(2) and 2.779(2) Å).[21b] In **5a** and **5b** both

(20) (a) Rhodes, L. F.; Huffman, J. C.; Caulton, K. G. *J. Am. Chem. Soc.* **1983**, *105*, 5137. (b) Bel'skii, V. K.; Ishchenko, V. M.; Bulychev, B. M.; Soloveichik, G. L. *Polyhedron* **1984**, *3*, 749. (c) Florke, U.; Haupt, H.-J. *Z. Kristallogr.* **1992**, *201*, 323.

(21) (a) Beringhelli, T.; Ciani, G.; D'Alfonso, G.; Freni, M.; Sironi, A. *J. Organomet. Chem.* **1985**, *295*, C7. (b) Connelly, N. G.; Howard, J. A. K.; Spencer, J. L.; Woodley, P. K. *J. Chem. Soc., Dalton Trans.* **1984**, 2003.

the Re−Cu and Re−Ag bonds are spanned by β-B−H→M interactions (B(4)−Cu = 2.169(3) Å and B(4)−Ag = 2.449(14) Å) involving boron atoms in the CCB*B*B coordinating face of the cage. Attachment of Cu(PPh$_3$) fragments to *closo*-3,1,2-MC$_2$B$_9$H$_{11}$ structures by both Cu−M and by either one or two B−H→Cu bonds is well-established,[4e,22] whereas complexes with any kind of B−H→Ag contacts are comparatively scarce.[22f,23] In fact **5b** is the first complex isolated where a carborane ligand η^5-7,8-C$_2$B$_9$H$_{11}$ bridges a metal−silver bond in such a manner. The coordination spheres about the copper and silver atoms are completed by the rhenium atom and by the PPh$_3$ ligand: Cu−P = 2.2051(8) Å and Ag−P = 2.373(3) Å, which are both within accepted ranges for M−P bonds of this nature.[24] The PPh$_3$ ligands lie transoid to the B(4) boron atoms of the agostic systems (B(4)−Cu−P = 161.88(9)°, B(4)−Ag−P = 171.1(3)°). The perturbation of the Re(CO)$_3$ group to accommodate the M(PPh$_3$) moieties appears to be slight, with the immediately adjacent (O)C−Re−C(O) angles only marginally widened (C(3)−Re−C(4) = 95.53(12)°, average C(3,4)−Re−C(5) = 85.1° (**5a**); C(3)−Re−C(5) = 93.4(5)°, average C(3,5)−Re−C(4) = 86.3° (**5b**)). This would seem to imply that the Re−M bonds primarily involve a rhenium 5d-based orbital, previously from a nonbonding set in the anion of **1**. Therefore, the M(PPh$_3$) units in **5** actually cause little electronic disruption to the Re(CO)$_3$(η^5-C$_2$B$_3$) core, requiring only slight steric accommodation. This is logically greater for Cu(PPh$_3$) (ca. 2°) than for Ag(PPh$_3$) because a larger cone angle for Cu(PPh$_3$) derives from the smaller atomic radius for copper.

With the solid-state structures of **5a**,**b** firmly established, the NMR spectroscopic data are clearly not in accord with the results of the X-ray structure determinations. Evidently in solution at ambient temperatures **5a**,**b** are highly dynamic. The NMR data can be accounted for by a mechanism which includes Re−M heterolytic fission and facile migration of the [M(PPh$_3$)]$^+$ fragments about the polyhedral cage surface, much like that described for the [Rh(PPh$_3$)$_2$]$^+$ unit in the complexes [5,10-(μ-H)$_2$-*exo*-{Rh(PPh$_3$)$_2$}-7,8-Me$_2$-*nido*-7,8-C$_2$B$_9$H$_8$] and [10-*endo*-{Au(PPh$_3$)}-5,10-(μ-H)$_2$-*exo*-{Rh(PPh$_3$)$_2$}-7,8-Me$_2$-*nido*-7,8-C$_2$B$_9$H$_7$].[11] A representative structure at any energy minimum along this dynamic profile probably involves at least two B−H→ligations to the [M(PPh$_3$)]$^+$ cation, possibly three. Measurement of the NMR spectra of both complexes **5** at −90 °C failed to reveal any quenching of this mobility.

Conclusion

In the syntheses of the complexes **5** we have shown that **1** can in limited circumstances be used as a synthon for the formation of metal−metal bonds. The existence of these complexes is incidentally supportive of the proposed Re−Rh-bonded species **B** in Scheme 1. We are currently investigating reactions of **1** with platinum complexes. Preliminary results show that Re−Pt bonds are formed and exist in solution at ambient temperatures. We have also demonstrated that the anion of **1** can function as a mono-, bi-, or tridentate ligand by virtue of the coordination of the carborane B−H bonds to exopolyhedral metal centers in complexes **4**, **3**, and **2**, respectively. Despite earlier negative results, and with some persistent probative effort, we have shown **1** to be as versatile a reagent as [N(PPh$_3$)$_2$]$_2$[Re(CO)$_3$(η^5-7-CB$_{10}$H$_{11}$)].[5]

Experimental Section

General Considerations. All experiments were conducted under an atmosphere of dry nitrogen using Schlenk tube techniques. Solvents were freshly distilled under nitrogen from appropriate drying agents before use. Light petroleum refers to that fraction of boiling point 40−60 °C. Chromatography columns (ca. 20 cm in length and 2 cm in diameter, unless otherwise stated) were packed with silica gel (Acros, 60−200 mesh). Celite pads used for filtration were ca. 3 cm in length and 2 cm in diameter. The NMR measurements were recorded at the following frequencies: ^{1}H at 360.13 MHz, ^{13}C at 90.56 MHz, ^{11}B at 115.55 MHz, and ^{31}P at 145.78 MHz. The salt Cs[Re(CO)$_3$(η^5-7,8-C$_2$B$_9$H$_{11}$)] (**1**) was synthesized using a modification of the procedure reported previously,[3] and this is detailed below. The reagents [NHMe$_3$][*nido*-7,8-C$_2$B$_9$H$_{12}$],[25] [ReBr(CO)$_5$],[26] [RuCl$_2$(PPh$_3$)$_3$],[27] [RhCl(PPh$_3$)$_3$],[28] [Fe(CO)$_2$(THF)(η-C$_5$H$_5$)][BF$_4$],[13] and [CuCl(PPh$_3$)$_3$][29] were made as previously described. The complexes [RuI(CO)$_2$(η-C$_5$H$_5$)] and [FeI(CO)$_2$(η-C$_5$Me$_5$)] were prepared using the same procedure as for [FeI(CO)$_2$(η-C$_5$H$_5$)].[30] Sodium hydride, supplied as a 60% dispersion in oil by Aldrich, was weighed out, washed with two portions of light petroleum (2 × 10 mL), and dried in vacuo immediately prior to use. The compound [Fe(η-C$_5$H$_4$PPh$_2$)$_2$] was purchased from Strem.

Improved Synthesis of Cs[Re(CO)$_3$(η^5-7,8-C$_2$B$_9$H$_{11}$)]. The compound [NHMe$_3$][*nido*-7,8-C$_2$B$_9$H$_{12}$] (0.50 g, 2.58 mmol) was dissolved in THF (20 mL) in a two-necked 100 mL round-bottom flask fitted with a condenser which in turn was connected to a Schlenk line. To this was carefully added a suspension of NaH (0.52 g, 21.67 mmol) in THF (30 mL). After the initial effervescence had subsided, the flask was stoppered and the suspension was heated to reflux for ca. 12 h. Immediately after this refluxing had commenced, the compound [ReBr(CO)$_5$] (1.00 g, 2.46 mmol) was placed in a second 250 mL two-necked round-bottom flask also fitted to a Schlenk line via a condenser (or in a large reflux Schlenk tube) and dissolved in THF (30 mL) and then heated to reflux, also for ca. 12 h. After this period had elapsed (usually overnight), the heat source was removed from the carborane/NaH suspension and the mixture cooled to room temperature. Once cooled, the stirring was ceased and the excess NaH allowed to settle. At this point the heat source was removed from the rhenium solution, though it should not be allowed to cool below ca. 55 °C. The solution of Na$_2$[*nido*-7,8-C$_2$B$_9$H$_{11}$] was taken up in a syringe (being careful not to disturb the settled NaH) and transferred to the [ReBr(CO)$_3$(THF)$_2$] solution with vigorous

(22) (a) Do, Y.; Knobler, C. B.; Hawthorne, M. F. *J. Am. Chem. Soc.* **1987**, *109*, 1853. (b) Kang, H. C.; Do, Y.; Knobler, C. B.; Hawthorne, M. F. *Inorg. Chem.* **1988**, *27*, 1716. (c) Cabioch, J.-L.; Dossett, S. J.; Hart, I. J.; Pilotti, M. U.; Stone, F. G. A. *J. Chem. Soc., Dalton Trans.* **1991**, 519. (d) Jeffery, J. C.; Stone, F. G. A.; Topaloğlu, I. *J. Organomet. Chem.* **1993**, *451*, 205. (e) Ellis, D. D.; Couchman, S. M.; Jeffery, J. C.; Malget, J. M.; Stone, F. G. A. *Inorg. Chem.* **1999**, *38*, 2981. (f) Ellis, D. D.; Franken, A.; Stone, F. G. A. *Organometallics* **1999**, *18*, 2362.

(23) (a) Colquhoun, H. M.; Greenhough, T. J.; Wallbridge, M. G. H. *J. Chem. Soc., Dalton Trans.* **1980**, 192. (b) Shelly, K.; Finster, D. C.; Lee, Y. J.; Scheidt, W. R.; Reed, C. A. *J. Am. Chem. Soc.* **1985**, *107*, 5955. (c) Eigenbrot, C. W.; Liston, D. J.; Reed, C. A.; Scheidt, W. R. *Inorg. Chem.* **1987**, *26*, 2739. (d) Park, Y.-W., Kim, J.; Do, Y. *Inorg. Chem.* **1994**, *33*, 1.

(24) Allen, F. H.; Brammer, L.; Kennard, O.; Orpen, A. G.; Taylor, R.; Watson, D. G. *J. Chem. Soc., Dalton Trans.* **1989**, S1.

(25) Hawthorne, M. F.; Young, D. C.; Garrett, P. M.; Owen, D. A.; Schwerin, S. G.; Tebbe, F. N.; Wegner, P. A. *J. Am. Chem. Soc.* **1968**, *90*, 862.

(26) Abel, E. W.; Wilkinson, G. *J. Chem. Soc.* **1959**, 1501.

(27) Hallman, P. S.; Stephenson, T. A.; Wilkinson, G. *Inorg. Synth.* **1970**, *12*, 238.

(28) Osborn, J. A.; Wilkinson, G. *Inorg. Synth.* **1967**, *10*, 67.

(29) Stephens, R. D. *Inorg. Synth.* **1979**, *19*, 87.

(30) Piper, T. S.; Wilkinson, G. *J. Inorg. Nucl. Chem.* **1956**, *2*, 28.

stirring. The resulting mixture was then refluxed for 5 h. After this time it is cooled to room temperature and the THF removed in vacuo. At this point it was no longer necessary to maintain anaerobic conditions. The residue was dissolved in water (50 mL) (some effervescence may occur) and then CsCl (0.80 g, 4.75 mmol) added. The product $Cs[Re(CO)_3(\eta^5\text{-}7,8\text{-}C_2B_9H_{11})]$ (**1**; 1.20 g, 91%) precipitated rapidly from solution as a creamy white solid and was collected by filtration and then dried in vacuo overnight at 100 °C.

Preparation of the Compound $[Re(CO)_3(\eta^5\text{-}2,3,10\text{-}(\mu\text{-}H)_3\text{-}exo\text{-}\{RuCl(PPh_3)_2\}\text{-}7,8\text{-}C_2B_9H_8)]$. The compounds **1** (0.05 g, 0.09 mmol) and $[RuCl_2(PPh_3)_3]$ (0.09 g, 0.09 mmol) were dissolved in CH_2Cl_2 (10 mL), and the mixture was stirred for 1 h. Over this time the solution turned dark orange and a pale precipitate formed. The suspension was filtered through Celite to remove precipitated CsCl, and the solvent volume was reduced in vacuo to ca. 5 mL. This solution was then chromatographed, and a red-orange band was eluted with neat CH_2Cl_2. Removal of solvent in vacuo followed by crystallization from CH_2Cl_2−light petroleum (10 mL, 2:3) gave red microcrystals of $[Re(CO)_3(\eta^5\text{-}2,3,10\text{-}(\mu\text{-}H)_3\text{-}exo\text{-}\{RuCl(PPh_3)_2\}\text{-}7,8\text{-}C_2B_9H_8)]$ (**2a**; 0.03 g). The major product **2a** is inseparable from its minor isomer **2b**.

Syntheses of the Complexes $[Re(CO)_3\{\eta^5\text{-}5,10\text{-}(\mu\text{-}H)_2\text{-}exo\text{-}(RhL_2)\text{-}7,8\text{-}C_2B_9H_9\}]$ ($L_2 = (PPh_3)_2$, $\{Fe(\eta\text{-}C_5H_4PPh_2)_2\}$). (i) To the compounds **1** (0.10 g, 0.19 mmol) and $[RhCl(PPh_3)_3]$ (0.17 g, 0.18 mmol) was added CH_2Cl_2 (15 mL) and the mixture stirred for 1 h. Solvent was reduced in volume in vacuo to ca. 2 mL and light petroleum (15 mL) added. The suspension was stirred for 1 h, after which time the solid was allowed to settle and the supernatant liquid removed using a syringe. The residue was washed with light petroleum (2 × 10 mL) and then dissolved in CH_2Cl_2 (10 mL) and filtered through Celite. Solvent was removed in vacuo and then CH_2Cl_2−light petroleum (5 mL, 2:3) introduced. This solution was then applied to the top of a chromatography column cooled to −30 °C. Elution with the same solvent mixture removed a red fraction from which solvent was removed in vacuo. Crystallization from CH_2Cl_2−light petroleum (10 mL, 1:4) yielded red microcrystals of $[Re(CO)_3(\eta^5\text{-}5,10\text{-}(\mu\text{-}H)_2\text{-}exo\text{-}\{Rh(PPh_3)_2\}\text{-}7,8\text{-}C_2B_9H_9)]$ (**3a**; 0.13 g).

(ii) The compounds $[RhCl(PPh_3)_3]$ (0.10 g, 0.11 mmol) and $[Fe(\eta\text{-}C_5H_4PPh_2)_2]$ (0.06 g, 0.11 mmol) were treated together with CH_2Cl_2 (10 mL) and stirred at room temperature for 1 h. Reduction of the volume of solvent in vacuo to ca. 1 mL was followed by addition of light petroleum (20 mL) and the suspension stirred for 2 h. The precipitate of $[RhCl\{Fe(\eta\text{-}C_5H_4PPh_2)_2\}(PPh_3)]$ so formed was allowed to settle, and the supernatant liquid was syringed off. The resulting residue was dried in vacuo for 5 min. The salt **1** (0.06 g, 0.11 mmol) was then added, followed by CH_2Cl_2 (10 mL), and the mixture stirred at room temperature for 2 h. The volume of solvent was reduced in volume in vacuo to ca. 2 mL, and light petroleum (20 mL) was added and the suspension stirred for 30 min. The supernatant liquid was again removed with a syringe from the settled precipitate, and the residue was treated with CH_2Cl_2 (10 mL) and the solution filtered through Celite. Solvent was removed in vacuo and CH_2Cl_2−light petroleum (5 mL, 1:1) added. This solution was then chromatographed at −30 °C, and elution with the same solvent mixture removed a red fraction. Solvent was removed in vacuo, and crystallization from CH_2Cl_2−light petroleum (10 mL, 1:4) gave red microcrystals of $[Re(CO)_3(\eta^5\text{-}5,10\text{-}(\mu\text{-}H)_2\text{-}exo\text{-}(Rh\{Fe(\eta\text{-}C_5H_4PPh_2)_2\})\text{-}7,8\text{-}C_2B_9H_9)]$ (**3b**; 0.07 g).

Syntheses of the Complexes $[Re(CO)_3(\eta^5\text{-}n\text{-}(\mu\text{-}H)\text{-}exo\text{-}\{M(CO)_2(\eta\text{-}C_5R_5)\}\text{-}7,8\text{-}C_2B_9H_{10})]$ ($M = Fe$, $R = H$, $n = 10$; $M = Ru$, $R = H$, $n = 10$; $M = Fe$, $R = Me$, $n = 9$, 10). (i) The salts **1** (0.43 g, 0.80 mmol) and $[Fe(CO)_2(THF)(\eta\text{-}C_5H_5)][BF_4]$ (0.27 g, 0.80 mmol) were treated with CH_2Cl_2 (10 mL), and the mixture was stirred for 20 min. The mixture was then filtered through Celite, following which solvent was removed in vacuo. The residue was taken up in CH_2Cl_2−light petroleum (5 mL, 1:1) and chromatographed, with the same solvent mixture as eluent. An orange fraction was obtained, from which solvent was removed in vacuo. The residue was crystallized from CH_2Cl_2−light petroleum (10 mL, 1:4) to give orange microcrystals of $[Re(CO)_3(\eta^5\text{-}10\text{-}(\mu\text{-}H)\text{-}exo\text{-}\{Fe(CO)_2(\eta\text{-}C_5H_5)\}\text{-}7,8\text{-}C_2B_9H_{10})]$ (**4a**; 0.46 g).

(ii) The complex $[RuI(CO)_2(\eta\text{-}C_5H_5)]$ (0.19 g, 0.54 mmol) was dissolved in THF (10 mL), and this mixture was treated with $AgBF_4$ (0.11 g, 0.57 mmol) and stirred for 30 min. The suspension was filtered through Celite, and the THF was then removed in vacuo. Compound **1** (0.30 g, 0.56 mmol) was added to this residue, followed by CH_2Cl_2 (10 mL), and the reaction mixture stirred for 2 h. Solvent was removed in vacuo and then CH_2Cl_2−light petroleum (5 mL, 1:1) added. This solution was chromatographed, with the same solvent mixture as eluent, to afford a small orange fraction, which was discarded. Further elution removed a yellow fraction. Solvent was removed in vacuo, and crystallization from CH_2Cl_2−light petroleum (10 mL, 1:9) gave a yellow solid, which could be recrystallized at −50 °C to give yellow microcrystals of $[Re(CO)_3(\eta^5\text{-}10\text{-}(\mu\text{-}H)\text{-}exo\text{-}\{Ru(CO)_2(\eta\text{-}C_5H_5)\}\text{-}7,8\text{-}C_2B_9H_{10})]$ (**4b**; 0.16 g).

(iii) Using a similar procedure, the compounds $[FeI(CO)_2(\eta\text{-}C_5Me_5)]$ (0.08 g, 0.21 mmol), **1** (0.10 g, 0.19 mmol), and $AgBF_4$ (0.04 g, 0.21 mmol) gave orange microcrystals of $[Re(CO)_3(\eta^5\text{-}n\text{-}(\mu\text{-}H)\text{-}exo\text{-}\{Fe(CO)_2(\eta\text{-}C_5Me_5)\}\text{-}7,8\text{-}C_2B_9H_{10})]$ ($n = 10$ (**4c**), 9 (**4d**); 0.11 g), formed as an inseparable mixture of isomers.

Preparation of the Complexes $[ReM(\mu\text{-}10\text{-}H\text{-}\eta^5\text{-}7,8\text{-}C_2B_9H_{10})(CO)_3(PPh_3)]$ ($M = Cu$, Ag). (i) The compounds **1** (0.10 g, 0.19 mmol) and $[CuCl(PPh_3)_3]$ (0.17 g, 0.19 mmol) were treated with CH_2Cl_2−THF (10 mL, 4:1), and the mixture was stirred for 1 h. Solvent was reduced in volume in vacuo to ca. 3 mL and light petroleum (20 mL) added. After 30 min of stirring the precipitate was allowed to settle and the supernatant liquid syringed off. This washing was repeated twice. The residue was then taken up in CH_2Cl_2−light petroleum (5 mL, 1:1) and the solution filtered through a silica gel plug (2 × 5 cm). As the desired product is colorless in solution, it is necessary to ascertain its presence in the eluant with monitoring by IR spectral measurements. Solvent was removed in vacuo and the residue crystallized from CH_2Cl_2−light petroleum (10 mL, 1:4) to yield white microcrystals of $[ReCu(\mu\text{-}10\text{-}H\text{-}\eta^5\text{-}7,8\text{-}C_2B_9H_{10})(CO)_3(PPh_3)]$ (**5a**; 0.08 g).

(ii) The compounds $AgBF_4$ (0.06 g, 0.31 mmol) and PPh_3 (0.08 g, 0.31 mmol) were treated with THF (10 mL), and the solution was stirred for 20 min. In a second Schlenk tube, fitted with a pressure-equalized dropping funnel, compound **1** (0.17 g, 0.32 mmol) was dissolved in THF and cooled to −80 °C. The solution of $[Ag(PPh_3)(THF)][BF_4]$ was transferred to the dropping funnel and added over 15 min. The funnel was then replaced by a stopper and the mixture, which becomes cloudy with no coloration, was gradually warmed to room temperature. Solvent was removed in vacuo and the residue taken up in CH_2Cl_2−light petroleum (5 mL, 1:1) and applied to a silica gel plug (2 × 5 cm). The product solution is again colorless, and it is necessary to monitor the eluant by consecutive IR measurements. Solvent was removed in vacuo and the residue crystallized from CH_2Cl_2−light petroleum (10 mL, 1:4) to give white microcrystals of $[ReAg(\mu\text{-}10\text{-}H\text{-}\eta^5\text{-}7,8\text{-}C_2B_9H_{10})(CO)_3(PPh_3)]$ (**5b**; 0.15 g).

Structure Determinations of Compounds 2a and 5a. Crystals of **2a** and **5a** were grown by diffusion of light petroleum into CH_2Cl_2 solutions of the complexes. All crystals were mounted on glass fibers, and low-temperature data were collected on a Siemens SMART CCD area-detector three-circle diffractometer (Mo Kα X-radiation, graphite monochromator, $\bar{\lambda} = 0.710\ 73$ Å). For three or four settings of φ, narrow data "frames" were collected for 0.3° increments in ω. For the monoclinic complex **2a** just over a hemisphere of data was collected, while for the triclinic crystals **5a** full spheres of data

Table 8. Data for X-ray Crystal Structure Analyses

	2a	4b	5a	5b
cryst dimens/mm	0.20 × 0.15 × 0.15	0.20 × 0.18 × 0.10	0.40 × 0.40 × 0.40	0.33 × 0.26 × 0.15
formula	$C_{41}H_{41}B_9ClO_3P_2ReRu$	$C_{12}H_{16}B_9O_5ReRu$	$C_{23}H_{26}B_9CuO_3PRe$	$C_{23}H_{26}AgB_9O_3PRe\cdot0.5CH_2Cl_2$
M_r	1063.69	624.81	728.44	815.23
cryst color, shape	red prism	yellow block	colorless cube	colorless block
cryst syst	monoclinic	monoclinic	triclinic	monoclinic
space group	$P2_1/n$	$P2_1/c$	$P\bar{1}$	$C2/c$
T/K	173(2)	293(2)	173(2)	293(2)
a/Å	19.4834(25)	14.461(2)	9.2246(20)	24.5808(27)
b/Å	12.3344(10)	10.380(4)	13.0494(13)	8.8020(19)
c/Å	19.7114(18)	14.694(2)	13.5816(16)	28.1287(44)
α/deg			63.439(7)	
β/deg	115.095(8)	114.266(13)	84.281(14)	102.190(11)
γ/deg			70.141(12)	
V/Å^3	4289.8(8)	2010.8(9)	1372.7(4)	5949
Z	4	4	2	8
d_{calcd}/g cm^{-3}	1.647	2.064	1.762	1.821
μ(Mo Kα)/mm^{-1}	3.347	6.785	5.264	4.894
F(000)/e	2088	1168	704	3128
2θ range/deg	4.0−55.0	3.2−45.0	3.4−55.0	3.4−45.0
no. of rflns measd	27067	2737	13708	3973
no. of indep rflns	9806	2577	6182	3869
R(int)	0.03	0.031	0.03	0.038
refln limits				
h	−25 to +22	−15 to 0	−11 to +11	−26 to 0
k	−16 to +13	0−12	−16 to +16	0−9
l	−24 to +25	−15 to +15	−17 to +17	−29 to +30
final residuals				
wR2[a]	0.052	0.091	0.037	0.095
R1[b]	0.025	0.039	0.019	0.048
weighting factors[a]				
a	0.0218	0.0451	0.0074	0.0272
b	0.0	0.0	0.0	3.8839
goodness of fit on F^2	0.97	1.076	0.91	1.077
final electron density diff features (max/min)/e Å^{-3}	0.818, −0.985	1.199, −1.130	0.845, −0.822	1.335, −0.670

[a] Structure was refined on F_o^2 using all data: wR2 = $[\sum[w(F_o^2 - F_c^2)^2]/\sum w(F_o^2)^2]^{1/2}$, where $w^{-1} = [\sigma^2(F_o^2) + (aP)^2 + bP]$ and $P = [\max(F_o^2,0) + 2F_c^2]/3$. [b] This value is given for comparison with refinements based on F_o with a typical threshold of $F_o > 4\sigma(F_o)$ and R1 = $\sum||F_o| - |F_c||/\sum|F_o|$ and $w^{-1} = [\sigma^2(F_o) + gF_o^2]$.

were collected. It was confirmed that crystal decay had not taken place during the course of the data collections. The substantial redundancy in data allows empirical absorption corrections (SADABS[31]) to be applied using multiple measurements of equivalent reflections. The data frames were integrated using SAINT;[31] structures were solved by conventional direct methods and refined by full-matrix least squares on all F^2 data using Siemens SHELXTL version 5.03.[31]

For both structures the non-hydrogen atoms were refined with anisotropic thermal parameters. Cage carbon atoms were identified from the magnitudes of their anisotropic thermal parameters and from a comparison of the bond lengths to adjacent boron atoms. The agostic B−H⇀M hydrogen atoms H(4), H(9), and H(10) in complex **2a** and H(4) in complex **5a** were located from final difference Fourier syntheses, and their positions and isotropic thermal parameters were refined. All other hydrogen atoms were included in calculated positions and allowed to ride on the parent boron or carbon atoms with isotropic thermal parameters (U_{iso} = 1.2[U_{iso}(parent atom)]). All calculations were carried out on Silicon Graphics Iris, Indigo, or Indy computers, and the experimental data are summarized in Table 8.

Structure Determinations of Compounds 4b and 5b. Crystals of **4b** and **5b** were grown by diffusion of light petroleum into CH_2Cl_2 solutions of the complexes. Those of **5b** grew with a half-molecule of CH_2Cl_2 in the asymmetric unit, the carbon residing on a 2-fold axis. Diffracted intensities were collected on an Enraf-Nonius CAD-4 operating in the ω−2θ (**4b**) or ω (**5b**) scan mode, using graphite-monochromated Mo Kα X-radiation ($\bar{\lambda}$ = 0.710 73 Å). For each structure, the final unit cell dimensions were determined from the setting angle values of 25 accurately centered reflections. The stability of the crystals during the period of the data collections was monitored by measuring the intensities of three standard reflections every 2 h. Data were collected at the following scan speeds: 4.13−5.17° min^{-1} in ω for **4b** with a scan range of (1.15 + 0.35 tan θ)°; and 5.17° min^{-1} in ω with a scan range of (1.15 + 0.34 tan θ)° for **5b**. The data were corrected for Lorentz, polarization, and X-ray absorption effects, the last by a semiempirical method based on azimuthal scans of ψ data of several Euclerian angles (χ) near 90°.

Structures were solved by direct methods (**4b**) or conventional heavy-atom methods (**5b**), and successive Fourier difference syntheses were used to locate all non-hydrogen atoms, using the SHELXTL-PC package.[31] Refinements were made by full-matrix least squares on F^2 data, using SHELXL-93,[31] with anisotropic thermal parameters for all non-hydrogen atoms. Cage carbon atoms were identified from the magnitudes of their anisotropic thermal parameters and from a comparison of the bond lengths to adjacent boron atoms. The hydride atom H(4) in **4b** and the agostic B−*H*⇀M hydrogen atom H(4) in **5b** were located in final difference Fourier syntheses, their coordinates freely refined, and isotropic thermal parameters fixed with U_{iso} = 0.05 Å^2 for **4b** and 1.2[U_{iso}(parent atom)] for **5b**. All other hydrogen atoms were included in calculated positions (C−H = 0.96 Å and B−H = 1.10 Å) and allowed to ride on their parent boron or carbon atom with fixed isotropic thermal parameters (U_{iso} = 1.2[U_{iso}(parent atom)]). Atomic scattering factors were taken from the usual source.[32] All

(31) Siemens X-ray Instruments, Madison, WI, 1995.

(32) *International Tables for X-ray Crystallography*; Kynoch Press: Birmingham, U.K., 1974; Vol. 4.

calculations were carried out on Dell PC computers, and the experimental data are summarized in Table 8.

Acknowledgment. We thank the Robert A. Welch Foundation for support (Grant AA-1201) and Dr. J. C. Jeffery for the use of X-ray facilities by D.D.E. at the University of Bristol, Bristol, U.K.

Supporting Information Available: Tables of atomic coordinates and *U* values, bond lengths and angles, and anisotropic thermal parameters and ORTEP diagrams for **2a**, **4b**, **5a**, and **5b** in CIF format and the ^{1}H NMR spectrum of **3a** measured at −90 °C. This material is available free of charge via the Internet at http://pubs.acs.org.

OM9905097